Online hemodiafiltration inhibits inflammation-related endothelial dysfunction and vascular calcification of uremic patients modulating miR-223 expression in plasma extracellular vesicles

On line-hemodiafiltration inhibits inflammation-related endothelial dysfunction and vascular calcification of uremic patients modulating miR-223 expression in plasma extracellular vesicles

†*Claudia Cavallari, ‡*Sergio Dellepiane, †Valentina Fonsato, ‡Davide Medica, §Marita Marengo, ¶Massimiliano Migliori, ||Alessandro D. Quercia, †Adriana Pitino, §Marco Formica, ¶Vincenzo Panichi, ‡Stefano Maffei, ‡Luigi Biancone, #Emanuele Gatti, ††Ciro Tetta, ‡Giovanni Camussi, ||Vincenzo Cantaluppi

†2i3T Scarl, University of Torino, Italy; ‡Nephrology, Dialysis and Kidney Transplantation Unit, Department of Medical Sciences, University of Torino, Italy; §Nephrology and Dialysis Unit, ASLCN1, Cuneo, Italy; ¶Nephrology and Dialysis Unit, Versilia Hospital, Camaiore (LU), Italy; #Department for Health Sciences and Biomedicine, Danube University, Krems, Austria; ††Unicyte AG, Oberdorf, Switzerland; ||Nephrology and Kidney Transplantation Unit and Center for Autoimmune and Allergic Diseases (CAAD), Department of Translational Medicine, University of Piemonte Orientale (UPO), Novara, Italy;

*CC and SD equally contributed

Running Title: On line-hemodiafiltration inhibits vascular dysfunction

Address correspondence: Prof. Vincenzo Cantaluppi, S.C.D.U. Nefrologia e Trapianto Renale, Universita' del Piemonte Orientale "A. Avogadro", Azienda Ospedaliera Universitaria Maggiore della Carita', Via Solaroli, 17- 28100, Novara, ITALY: vincenzo.cantaluppi@med.uniupo.it.

Disclosures

This study was supported by a grant from Società Italiana di Nefrologia (SIN) "Progetti Ricerca Scientifica", Fondazione Cassa di Risparmio di Cuneo and Fondazione Cariplo, Local University Grants (UPO).

ABSTRACT

Decreased inflammation and cardiovascular mortality is evident in patients with end stage chronic kidney disease (CKD) treated by on-line hemodiafiltration (OL-HDF). Extracellular vesicles (EV) are mediators of cell-to-cell communication and contain different RNA types. This study investigated whether mixed OL-HDF (mOL-HDF) beneficial effects associate with changes in the RNA content of plasma EV in CKD patients. Thirty bicarbonate hemodialysis (BHD) patients were randomized 1:1 to continue BHD or switch to mOL-HDF. Concentration, size, and microRNA content of plasma EV were evaluated for 9 months; we then studied EV effects on inflammation, angiogenesis and apoptosis of endothelial cells (HUVEC), and on osteoblast mineralization of vascular smooth muscle cells (VSMC). mOL-HDF treatment reduced different inflammatory markers including circulating CRP, IL6 and NGAL. All hemodialysis patients showed higher plasma levels of endothelial-derived EV than healthy subjects, with no significant differences between BHD and mOL-HDF. However, BHD-derived EV had an increased expression of the pro-atherogenic miR-223 in respect to healthy subjects or mOL-HDF. Compared to EV from healthy subjects, those from hemodialysis patients reduced angiogenesis, increased HUVEC apoptosis and VSMC calcification; however, all these detrimental effects were reduced with mOL-HDF in respect to BHD. Cell transfection with miR-223 mimic or antagomiR proved the role of this miRNA in EV-induced HUVEC and VSMC dysfunction. The switch from BHD to mOL-HDF significantly reduced systemic inflammation and miR-223 expression in plasma-EV, thus improving HUVEC angiogenesis and reducing VSMC calcification.

INTRODUCTION

Dialysis patients suffer from a high mortality, mostly related to vascular events (1, 2). Recently, several studies demonstrated an improvement of inflammatory parameters and of cardiovascular outcomes in patients with end stage chronic kidney disease (CKD) treated by on-line hemodiafiltration (OL-HDF) (3–5). This cardio-protective effect may be ascribed to an enhanced clearance of middle molecules involved in CKD-associated inflammation, endothelial dysfunction and vascular calcification (2, 6–8).

Increasing evidences indicate that plasma extracellular vesicles (EV) contribute to several physiological and pathological processes (9, 10). EV act as intercellular mediators by shuttling lipids, proteins and predominantly extracellular RNAs (11, 12). Indeed, several biological activities of EV may be ascribed to the transfer of microRNAs (miRNAs), small noncoding RNAs able to regulate post-transcriptional expression of gene products (13). EV-carried miRNAs are protected from the activity of degrading enzymes allowing their persistence in biological fluids and their delivery at distant sites. Recent studies have shown that plasma EV exert pro-inflammatory and pro-thrombotic properties and that EV may modulate endothelial function, suggesting a potential role of these microparticles in the pathogenesis of inflammatory disorders and atherosclerosis (14). Moreover, both EV and miRNAs circulating in the bloodstream reflect tissue damage and may be considered as biomarkers of disease activity (11, 15–18). Increased plasma levels of EV have been reported in hemodialysis patients in association with inflammatory parameters such as CRP and IL-6 (19). However, it remains unclear whether the dialysis procedure itself may affect the release of EV and the potential pathogenic role of EV-carried miRNAs in inflammation and vascular damage has not been fully elucidated. We herein hypothesized that circulating EV play a major role in dialysis associated vascular dysfunction and that OL-HDF is beneficial to the vascular system also by modulating the circulating EV content of RNA.

The aims of the present study were: 1) to isolate and characterize plasma EV derived from patients with end stage chronic kidney disease (CKD) undergoing high flux bicarbonate hemodialysis

74 (BHD) before and after switching to mixed on-line haemodiafiltration (mOL-HDF); 2) to analyze if
75 different dialysis modalities modulate EV-miRNAs potentially involved in inflammation,
76 endothelial dysfunction, atherosclerosis and vascular calcification.
77

PATIENTS AND METHODS

Patients

Thirty patients undergoing regular high flux bicarbonate hemodialysis (BHD) were enrolled in the study. Written informed consent was obtained. The study was conducted in accordance to Helsinki declaration, approved by the Ethic Committee of the "Città della Salute e della Scienza di Torino" University Hospital (Cod. 0030959, CEI/568) and registered in Clinicaltrials.gov (ID: NCT03202212). Inclusion criteria were: age >18 yrs., hemodialysis from at least 6 months (3 times for week), blood flow rate (Qb) ≥250 ml/min using arteriovenous fistula (AVF) or permanent central venous catheter (CVC), blood creatinine clearance <5 ml/min, urine output <500 ml/die. Exclusion criteria were: neoplastic diseases, autoimmune diseases, solid organ or bone marrow transplantation. Enrolled patients were randomized to continue high flux bicarbonate hemodialysis (BHD, n=15), or to switch to mixed on-line hemodiafiltration (mOL-HDF using FX 1000 CorDiax, Fresenius Medical Care, Bad Homburg, Germany; n=15) for 9 months (20). All enrolled patients completed the study with valid data (Figure 1). Immediately before the randomization (T0) and at 3 (T1), 6 (T2) and 9 (T3) months after study start, the following parameters were evaluated: blood flow rate (ml/min), dialysate flow rate (ml/hr), transmembrane pressure (TMP, mmHg), convective volume exchange (L/session), net ultrafiltration (L/session), dialysis time (minutes) white blood cell count, hemoglobin, hematocrit, C reactive protein (CRP), serum iron, transferrin saturation, ferritin, ERI (Epo units/Kg/week/hemoglobin), β2-microglobulin, homocysteine, calcium, phosphate, parathyroid hormone (PTH), Neutrophil Gelatinase-Associated lipocalin (NGAL). Dialysis adequacy was defined by eKt/V (according to Daugirdas formula) with a target value of 1.2. In mOL-HDF sessions a total convective volume >25 liters was considered as appropriate.

Patients' plasma was collected at the beginning of the second dialysis session of the week at T0, T1, T2 and T3. Harvested samples were used to perform nanoparticle tracking analysis (21), Guava FACS, western blot analysis, cellular and molecular biology studies; plasma drawn from healthy subjects was used as negative control. Clinical and laboratory parameters of the enrolled patients

were validated in a further cohort of hemodialysis patients treated by BHD (n=50) or post-dilution OL-HDF (n=30), peritoneal dialysis patients (n=10) and patients with stage IV CKD according to K-DOQI criteria (n=20).

Plasma collection and extracellular vesicle (EV) isolation

Patient and healthy control plasma was obtained by centrifuging peripheral blood in EDTA tubes at 6,000 g for 15 minutes at 20ºC. To isolate EVs, plasma samples were further centrifuged at 6,000 g for 20 minutes to remove remaining debris and then ultra-centrifuged at 100,000 g for 1h at 4ºC. EV were re-suspended in 500 µl of RPMI with 1% DMSO and stored at -80ºC.

Nanoparticle tracking analysis

EV preparations were diluted (1:1000) in sterile 0.9% saline solution and analyzed by NanoSight LM10 (Nanosight Ltd., Amesbury, UK) equipped with the Nanoparticle Analysis System & NTA 1.4 Analytical Software. The number of total EVs for each patient was obtained by multiplying the value given by the instrument (microparticles/ml) for the dilution made for the analysis and for the number of ml in which EVs were re-suspended.

Guava FACS Analysis

FACS analysis was performed on EV isolated from plasma by ultracentrifugation with GUAVA (GUAVA Easy-Cyte, Millipore) for the following markers: exosomes (CD9, CD63, CD81, CD86), platelets (CD41, CD42b, CD62P), monocytes/macrophages (CD14, CD15), leukocytes (CD45), B-cells (CD5, CD19, CD40), endothelial cells (CD31, CD105, CD144, CD146), T-cells (CD3) and different markers involved in atherosclerosis and vascular senescence (Tissue Factor, C5b-9, CD40-Ligand, ICOS, Fas-Ligand) (22, 23). Briefly, EVs were labeled with fluorescence-conjugated antibodies for 30 min at RT. EVs were washed twice in PBS with 0.5% BSA and resuspended in PBS 0.1% BSA. EVs were analyzed using Guava Incyte™ Software version 3.1.1 (M Millipore). The acquired data files were analyzed firstly by adding a EV-gate based on morphologic characteristics (FSC/SSC) and subsequently by the use of the lineage-specific markers. FITC or PE mouse non-immune isotypic IgG (Beckton Dickinson, USA) were used as controls..

Electronic molecular network generation: Protein Quest

To detect relevant miRNAs, electronic literature screening was performed by the apposite web platform Protein Quest (PQ – Biodigital Valley, Aosta, Italy). PQ retrieves all biological and medical information from PubMed abstract and captions, free articles, US patents and Clinical Trials. Moreover, it classifies terminology by mesh biomedical dictionary and elaborates hierarchic networks displaying term relationships. By using an appropriate research string, we selected all available articles and abstracts regarding uremic vascular dysfunction or calcification; afterwards PQ recognized all described miRNAs and relative pathways.

Western Blot Analysis

EV Proteins from 4 healthy individuals, 4 BHD and 4 mOL-HDF patients were extracted using the RIPA buffer (Sigma), supplemented with proteases and phosphatase inhibitors (Sigma) and then quantified using the Bradford assay (Biorad). Briefly, 10 µg of EV proteins were subjected to SDS-PAGE, transferred onto nitrocellulose membranes and underwent immunoblotting with antibodies directed to anti-CD63 (1:200, Santa Cruz), anti-CD9 (1:2000, Abcam) and normalized to Actin (1:200, Santa Cruz). The same procedure was followed for HUVEC treated with EV from the different experimental groups using IGF1R antibody (1:200, Santa Cruz).

Cell culture

Human umbilical vein-derived endothelial cells (HUVEC) were obtained by ATCC (PCS-100- 010-ATCC, Manassas VA). HUVEC were plated with EBM medium supplemented with 10% fetal calf serum (FCS – GE Health Care, Boston MA) and different endothelial growth factors as previously described (24). Human Vascular Smooth Muscular Cells (VSMC) were obtained by ATCC (CRL-1999, ATCC) and grown in Dulbecco Modified Eagle Medium (DMEM – GE Health Care) with 10% of FCS. Both cell types represent an accepted standard to investigate vascular uremic dysfunction (25–28).

RNA extraction and quantitative RT-PCR

Total RNA from HUVEC, VSMC or patients' EV, was extracted using mirVana kit (Life Technologies, USA), and analyzed by NanoDrop1000 spectrophotometer; samples of absorbance at 260/280 nm between 1.8 and 2.0 were adopted. We evaluated RUNX2 mRNA expression in VSMC by using High cDNA Reverse Transcription Kit and the Power SYBR Green PCR Master Mix on StepOnePlus Real Time System (Applied Biosystems, USA). We used the web platform Protein Quest (Biodigital Valley, Italy) to electronically screen the literature and to identify miRNA associated with uremic vascular dysfunction. Identified miRNA were detected in patients' EV using miScript Reverse Transcription Kit and miScript SYBR Green PCR Kit (Qiagen): 1ml of blood was used for each quantification experiment. Primers of the selected miRNA (hsa-miR-17-5p, -92-a, -223, -423-5p, -451a), RUNX2 and housekeeping transcripts (actin-β and RNU48) are displayed in Supplemental Table 1. Change in RNA expression was calculated using the $2^{-\Delta\Delta Ct}$ method. The miR-223 content was also analyzed in HUVEC or VSMC after transfection with specific mimic or antagomiR.

In vitro angiogenesis of endothelial cells

HUVEC were seeded into Matrigel coated wells (1,5 x 10^4 cells/well) in EBM with or without patients' EVs. VEGF (10 ng/ml) and uremic toxins (ADMA 10 μg/ml, p-cresyl sulphate 1 μg/ml and indoxyl sulphate 10 μg/ml) were used as positive or negative control, respectively. Experimental results were recorded with a Nikon-inverted microscope after 24 hours of incubation with different stimuli at 37º C. Image analysis of capillary-like structures was performed using the ImageJ Analysis System. Results were given as average number of capillary-like structures/field ±1SD (magnification x10). In all the assays, cells were stimulated with EV isolated from 1 ml of patients' blood for each 10 ml of medium.

In vitro apoptosis of endothelial cells

HUVEC were cultured in 96 flat-bottom microtiter plates at a concentration of 2 x 10^4 cells/well. Cells were examined after 24 hours of stimulation at 37ºC. VEGF and uremic toxins were used as negative or positive control, respectively. HUVEC were re-suspended in 100 μl of RPMI 1% BSA,

then mixed with 100 µl of Muse Annexin V & Dead Cell reagent, incubated for 20 min RT, and analyzed by the Muse Cell Analyzer (Millipore). In all the assays, cells were stimulated with EV isolated from 1 ml of patients' blood for each 10 ml of medium.

Osteoblastic differentiation of vascular smooth muscle cells (VSMC)

Vascular smooth muscle cells (VSMC) were fixed in 50% ethanol at RT for 10 min, stained with 10 mg/ml alizarin red for 5 min and washed twice in PBS. Retained dye was extracted with a solution of 20% methanol and 10% acetic acid; the absorbance at 450 nm was then measured (29).

Cell transfection

Transfection of miR-223 mimic (10 nM) or miR-223 inhibitor (100 nM) was performed on HUVEC or VSMC using HiPerfect Transfection method (Qiagen, Valencia, USA). The expression of miR-223 was evaluated by qRT-PCR. Data were expressed as Log of Rq, normalized to RNU-48.

Direct transfection of miR-223 inhibitor was performed co-incubating miR-223 inhibitor and BHD-EV followed by HUVEC or VSMC treatment. Angiogenesis and calcification effects were evaluated as reported.

Statistical analysis

Unless otherwise indicated, all data are shown as mean ± SEM. Statistical analysis was performed using the unpaired Student's t-test, ANOVA, or Kruskal-Wallis test when appropriate. A two-sided value of $p=0.05$ was considered significant.

RESULTS

Clinical and dialysis parameters

The main clinical characteristics of enrolled patients are described in Table I: no significant differences were found between BHD and mOL-HDF patients in terms of gender, age, prevalence of hypertension, diabetes and cardiovascular diseases, dialysis vintage and vascular access type.

As expected from previously published randomized clinical trials, the switch from BHD to mOL-HDF was associated with an improvement of inflammatory parameters: indeed, we observed a significant decrease in plasma CRP ($p=0.05$), ferritin ($p=0.04$), IL6 ($p<0.001$) and NGAL ($p=0.007$) in mOL-HDF patients between T0 and T1 (Figure 2). Consistently, the modulation of the inflammatory state was confirmed by the improvement of erythropoietin resistance index (ERI) ($p=0.05$). A decrease of β2-microglobulin not reaching statistical significance ($p=0.12$) was also observed. No significant differences were found in hemoglobin levels, transferrin saturation and homocysteine (not shown). By contrast, patients maintained in BHD did not show significant changes in any of the measured parameters. To exclude possible confounding factors, we also analyzed different clinical/therapeutic variables including nutritional and hemodynamic status, serum levels of calcium, phosphate and PTH, intravenous use of iron, treatment with statins, RAAS antagonists or vitamin D (reported in detail in Table II) and intradialytic variables (filter surface, heparin dose, treatment duration, blood and dialysis solution flow, transmembrane pressure, dialysis efficiency and convective volumes reported in details in Table III) at all the time points considered. As expected, mOL-HDF treatment was associated with a higher transmembrane pressure and with an improved eKt/V. All the other variables were comparable in the 2 groups at all considered time points.

Analysis of plasma EV

At study admission (T0), dialysis patients showed higher plasma EV concentration than healthy subjects and EV concentration did not change through the study time points within the groups (Figure 3A). EV size distribution showed similar results among the different groups with a mean

size of 170 nm (Figure 3B). Moreover, EV expressed typical exosomal markers such as CD9 and CD63 (Figure 3C). Results concerning EV concentration were confirmed in a further cohort of 80 patients undergoing chronic hemodialysis (n=50 in BHD and n=30 in post-dilution OL-HDF), 10 patients in peritoneal dialysis and 20 patients with K-DOQI stage IV CKD. Hemodialysis patients were further classified according to vascular access type (AVF vs. CVC): all groups were matched for age and gender. CKD stage IV and all peritoneal and hemodialysis patients showed a 5-fold increase of circulating plasma EV in comparison to healthy subjects (Figure 3D).

Guava FACS analysis of EV from dialysis patients at T0 revealed that the majority of circulating microparticles derived from platelets, monocytes/macrophages and endothelial cells; only endothelial EV were upregulated in comparison to healthy subjects (Figure 4A and Supplemental Fig. 1). In both groups, no changes in terms of cell-specific markers were found across the study time points (not shown). Of interest, plasma EV of enrolled patients expressed surface markers involved in inflammation, atherosclerosis, complement and coagulation activation (CD40-Ligand, ICOS, Fas-Ligand, C5b-9, Tissue Factor - Figure 4B and Supplemental Fig. 2). Consistently, an increased percentage of endothelial-derived particles was observed in all the different control groups (stage IV CKD, peritoneal dialysis or hemodialysis independently from vascular access type or dialysis modality - Figure 4C).

Characterization of microRNA content of plasma EV

By Protein Quest analysis (Figure 5A), 5 different miRNAs involved in endothelial dysfunction and vascular calcification were identified (miR-17-5p, miR-92a, miR-223, miR-423-5p, miR-451). The expression of these miRNAs was analyzed through all the study time points by qRT-PCR. The expression of miR-17-5p, miR-92a, miR-423-5p, miR-451 was not significantly different among healthy control, BHD- and mOL-HDF-derived EV (Figure 5B-E). By contrast, EV derived from dialysis patients showed an increased expression of miR-223 at T0 if compared to healthy controls; subsequently, mOL-HDF patients displayed a significant decline of EV miR-223 expression that was not observed in BHD patients and was maintained at all the time points considered (Figure 5F).

Patients from the control cohort treated by post-dilution OL-HDF had reduced levels of EV-carried miR-223 if compared to stage IV CKD patients, peritoneal dialysis patients and BHD-treated patients (Figure 5G).

Role of plasma EV-carried miR-223 in endothelial dysfunction

Since we identified a decreased expression of miR-223 in EV derived from mOL-HDF patients in respect to BHD patients, we performed *in vitro* experiments to evaluate the specific role of this miRNA in endothelial dysfunction. In respect to EV collected from healthy subjects, BHD-derived EV reduced the formation of capillary-like structures by HUVEC (Figure 6A). This anti-angiogenic effect was similar to what observed in presence of known uremic toxins (ADMA, p-cresyl sulphate, indoxyl sulphate). HUVEC angiogenesis was significantly higher with mOL-HDF-derived EV than with BHD-EV, even if not reaching the level observed with healthy EV. Similar results were also observed in experiments aimed to evaluate HUVEC apoptosis (Figure 6B).

To investigate whether miR-223 was involved in the anti-angiogenic and pro-apoptotic activities of plasma-EV, we evaluated the effect of specific mimic and antagomiR transfection, respectively. HUVEC transfected with mimic miR-223 showed a significant reduction of *in vitro* angiogenic response when challenged with healthy plasma-EV as well as with EV derived from dialysis patients. Conversely, transfection of HUVEC with miR-223-antagomiR significantly restored the angiogenic potential of plasma-EV, particularly in presence of BHD-derived EV (Figure 6C). The levels of expression of miR-223 in all experimental conditions were verified by qRT-PCR (Supplemental Fig. 3). Transfection of AntagomiR-223 was also used in order to inhibit miR-223 directly in BHD-EV. As shown in Figure 6D, transfected BHD-EV significantly restored pro-angiogenic properties on target cells indicating that EV can deliver miR-223.

Role of plasma EV-carried miR-223 in vascular smooth muscle cell calcification

We also investigated the role of EV-carried miR-223 in osteoblastic differentiation of VSMC. As shown by red alizarin staining and RUNX2 expression, EV derived from BHD patients induced an increase of VSMC calcification (Figure 7A, B, C). By contrast, EV derived from mOL-HDF

patients did not increase VSMC osteoblastic differentiation when compared to healthy subject particles. VSMC transfected with mimic miR-223 showed an increase of osteoblastic differentiation when incubated with healthy plasma-EV as well as with plasma-EV derived from BHD and mOL-HDF patients. Conversely, transfection of VSMC with miR-223-antagomiR significantly reduced the calcification potential of plasma-EV, particularly in presence of BHD derived EV (Figure 7D). Moreover, direct transfection of miR-223-inhibitor in BHD-EV led to a significant decrease of calcification potential induced by BHD-EV (Figure 7E).

Evaluation of miR-223 target genes

To investigate the role of miR-223 in endothelial dysfunction, we analyzed the potential target genes in HUVEC. The network predicted by IPA for miR-223 showed IGF1R as the most likely target (Figure 8A). We then evaluated whether miR-223 delivered by BHD-EV may modulate IGF1R expression in HUVEC. Western blot analysis demonstrated that treatment of HUVEC with BHD-EV significantly reduced IGF1R expression when compared to cells stimulated with BHD-EV + inhibitor-miR-223 (Figure 8B, C). A similar decrease was also observed when HUVEC were incubated with mimic-223, thus confirming miR-223 action on IGF1R. Although a previous study suggested β1-integrin as a further miR-223 target, we did not find any expression change of this protein in HUVEC (not shown) (30).

DISCUSSION

In this study, we evaluated the quantitative and qualitative changes of plasma EV in a population of patients with end stage CKD after switching from high flux BHD to mOL-HDF. We found that mOL-HDF was associated with a modulation of EV miR-223; additionally, our *in vitro* data suggested a role of miR-223 in CKD-related endothelial dysfunction and vascular calcification. As already reported in previous studies (2, 5–7), the use of a mixed convective-diffusive hemodepuration led to a significant decrease of inflammatory parameters such as CRP, ferritin, IL6, NGAL and erythropoietin resistance index (ERI). NGAL is a 25 KDa protein belonging to the calycin family that has been proposed as marker of inflammation and reduced iron bioavailability in hemodialysis patients (31, 32).

Systemic inflammation is a hallmark of CKD and plays a key role in the development and progression of cardiovascular diseases. HDF with high convection volumes is currently considered the most effective technique for achieving a better clearance of middle molecules in patients with end stage CKD (5). Several studies have shown that HDF improves intradialytic hemodynamic stability and some CKD complications such as inflammation, malnutrition, erythropoietin resistant anemia, and dialysis-associated amyloidosis. Large observational studies (DOPPS, Euclid, Riscavid) and RCT (Eshol) demonstrated an improved overall and cardiovascular survival in patients treated with HDF vs. BHD (7, 8, 33, 34). Basing on these studies, higher convective volumes are probably responsible for an enhanced clearance of middle/large uremic toxins involved in the development of cardiovascular complications and anemia (35). Post-dilution HDF is the most efficient infusion mode to maximize clearance of small and large solutes; nevertheless, this approach increases the frequency of technical problems due to hemoconcentration and high transmembrane pressure. The simultaneous use of pre- and post-dilution offered by mOL-HDF may avoid the disadvantages of traditional infusion modes. Indeed, in mOL-HDF pre and post-infusion percentage is automatically regulated through transmembrane pressure and ultrafiltration feedback (36). Recent studies compared the clearance of small, medium-sized and protein-bound molecules

and the convective volume administered in standard post-dilution OL-HDF vs. mOL-HDF without finding any significant difference. Moreover, mOL-HDF allows achieving a satisfactory convective volume exchange even in patients with suboptimal blood flow rates due to vascular access problem (20).

The influence of uremia-related inflammation on circulating plasma EV has been poorly investigated. It is well established that EV represent an important vehicle of intercellular communication due their ability in transporting molecules such as proteins, surface receptors, lipids, mRNA and, particularly, miRNA (11, 37). A significant increase of plasma EV is associated with several inflammatory diseases characterized by endothelial dysfunction and vascular calcification (19). In the present study, we found that CKD patients treated by high flux BHD or mOL-HDF presented higher levels of plasma EV when compared to healthy subjects matched for age and gender. Moreover, the analysis of surface antigens revealed the increase of EV expressing typical endothelial markers, suggesting the presence of ongoing microvascular damage. Furthermore, EV surface protein analysis revealed the presence of molecules involved in coagulation and complement cascades (Tissue Factor, C5b-9) and in the pathogenic mechanisms of inflammation and atherosclerosis: CD40-Ligand, ICOS and Fas-Ligand. These latter receptors are deeply involved in destabilization of atherosclerotic plaques: ICOS/ICOS-Ligand activation has been recently shown to play a key role in the pro-atherogenic activation of the T follicular / B-cell axis (38); similarly, both CD40 and CD40-Ligand are largely expressed in atherosclerotic plaques and in vascular calcifications of uremic patients (22, 39). In addition, the blockade of CD40/CD40-Ligand pathway led to a significant reduction of vascular damage in atherosclerosis-prone mice (40). Last, our research group previously demonstrated that soluble CD40-Ligand levels are predictive of combined cardiovascular morbidity and mortality in dialysis patients (41). Basing on these considerations, one could speculate that CD40-Ligand, ICOS and Fas-Ligand expressed by uremic EV may directly activate the counter-receptors expressed on endothelial cells and smooth muscle cells, leading to plaque destabilization. However, different studies showed that the biological

activities of EV are mainly ascribed to the transfer of RNA to target cells (37, 42, 43). In the present study, although we did not detect any significant difference between the two dialysis modalities in terms of concentration, size and surface antigens, we observed that EV isolated after switching to mOL-HDF presented a variation of miRNA content. Of interest, after the switch to mOL-HDF we found a decreased expression of miR-223 which is potentially involved in endothelial dysfunction and vascular calcification (31, 44–49) and is considered a biomarker of atherosclerosis progression (45, 50). Indeed, miR-223 inhibits angiogenesis by targeting β1-integrin and by preventing insulin like growth factor 1 signaling in endothelial cells (30); moreover, a recent study reported that miR-223 is also involved in osteoblast differentiation of VSMC (51).

The decrease of EV miR-223 found in mOL-HDF group was also observed in another cohort of hemodialysis patients regularly treated by post-dilution OL-HDF: this reduction was independent from the vascular access type and not observed in peritoneal dialysis patients and BHD-treated patients. These findings suggest that high volume HDF is responsible for modulation of pro-inflammatory and pro-atherogenic miRNA expression within plasma EV.

Furthermore, in our *in vitro* experiments, the increased expression of miR-223 in EV from BHD patients was associated with HUVEC angiogenesis inhibition, increased endothelial apoptosis and enhanced VSMC calcification. Of note, all these detrimental effects were down regulated by mOL-HDF. Consistently, experiments based on miR-223 mimic or antagomiR confirmed the relevance of this transcript in the biological activity of BHD-derived EV. Finally, we found that EV-carried miR-223 may modulate different intracellular pathways involved in endothelial angiogenesis and apoptosis including IGF1R, as suggested by IPA network analysis.

In conclusion, the results of the present study indicate that EV derived from hemodialysis patients express surface proteins and carry miRNAs involved in inflammation-related endothelial dysfunction and vascular calcification. Switching from BHD to mOL-HDF significantly decreased the expression of EV miR-223 but not of other miRNAs. The *in vitro* experiments indicated that the reduced expression of miR-223 justifies, at least partially, the decreased detrimental effect of

374 plasma EV from mOL-HDF patients. These results may contribute to explain the protective effects
375 on endothelial dysfunction and vascular calcification observed in OL-HDF clinical studies.
376

Acknowledgments

None

REFERENCES

1. Gai, M., I. Merlo, S. Dellepiane, V. Cantaluppi, G. Leonardi, F. Fop, C. Guarena, G. Grassi, and L. Biancone. 2014. Glycemic pattern in diabetic patients on hemodialysis: continuous glucose monitoring (CGM) analysis. *Blood Purif.* 38: 68–73.

2. Maduell, F., F. Moreso, M. Pons, R. Ramos, J. Mora-Macià, J. Carreras, J. Soler, F. Torres, J. M. Campistol, A. Martinez-Castelao, and ESHOL Study Group. 2013. High-efficiency postdilution online hemodiafiltration reduces all-cause mortality in hemodialysis patients. *J. Am. Soc. Nephrol. JASN* 24: 487–497.

3. den Hoedt, C. H., M. L. Bots, M. P. C. Grooteman, N. C. van der Weerd, A. H. A. Mazairac, E. L. Penne, R. Levesque, P. M. ter Wee, M. J. Nubé, P. J. Blankestijn, M. A. van den Dorpel, and CONTRAST Investigators. 2014. Online hemodiafiltration reduces systemic inflammation compared to low-flux hemodialysis. *Kidney Int.* 86: 423–432.

4. Grooteman, M. P. C., M. A. van den Dorpel, M. L. Bots, E. L. Penne, N. C. van der Weerd, A. H. A. Mazairac, C. H. den Hoedt, I. van der Tweel, R. Lévesque, M. J. Nubé, P. M. ter Wee, P. J. Blankestijn, and CONTRAST Investigators. 2012. Effect of online hemodiafiltration on all-cause mortality and cardiovascular outcomes. *J. Am. Soc. Nephrol. JASN* 23: 1087–1096.

5. Panichi, V., G. M. Rizza, S. Paoletti, R. Bigazzi, M. Aloisi, G. Barsotti, P. Rindi, G. Donati, A. Antonelli, E. Panicucci, G. Tripepi, C. Tetta, R. Palla, and RISCAVID Study Group. 2008. Chronic inflammation and mortality in haemodialysis: effect of different renal replacement therapies. Results from the RISCAVID study. *Nephrol. Dial. Transplant. Off. Publ. Eur. Dial. Transpl. Assoc. - Eur. Ren. Assoc.* 23: 2337–2343.

6. Ok, E., G. Asci, H. Toz, E. S. Ok, F. Kircelli, M. Yilmaz, E. Hur, M. S. Demirci, C. Demirci, S. Duman, A. Basci, S. M. Adam, I. O. Isik, M. Zengin, G. Suleymanlar, M. E. Yilmaz, M. Ozkahya, and Turkish Online Haemodiafiltration Study. 2013. Mortality and cardiovascular events in online haemodiafiltration (OL-HDF) compared with high-flux dialysis: results from the Turkish OL-HDF

Study. *Nephrol. Dial. Transplant. Off. Publ. Eur. Dial. Transpl. Assoc. - Eur. Ren. Assoc.* 28: 192–202.

7. Pérez-García, R. 2014. On-line haemodiafiltration after the ESHOL study. *Nefrol. Publ. Of. Soc. Esp. Nefrol.* 34: 139–144.

8. Panichi, V., A. Scatena, A. Rosati, R. Giusti, G. Ferro, E. Malagnino, A. Capitanini, A. Piluso, P. Conti, G. Bernabini, M. Migliori, D. Caiani, C. Tetta, A. Casani, G. Betti, and F. Pizzarelli. 2015. High-volume online haemodiafiltration improves erythropoiesis-stimulating agent (ESA) resistance in comparison with low-flux bicarbonate dialysis: results of the REDERT study. *Nephrol. Dial. Transplant. Off. Publ. Eur. Dial. Transpl. Assoc. - Eur. Ren. Assoc.* 30: 682–689.

9. Budaj, M., Z. Poljak, I. Ďuriš, M. Kaško, R. Imrich, M. Kopáni, L. Maruščáková, and I. Hulín. 2012. Microparticles: a component of various diseases. *Pol. Arch. Med. Wewnętrznej* 122 Suppl 1: 24–29.

10. Piccin, A., W. G. Murphy, and O. P. Smith. 2007. Circulating microparticles: pathophysiology and clinical implications. *Blood Rev.* 21: 157–171.

11. Camussi, G., M. C. Deregibus, S. Bruno, V. Cantaluppi, and L. Biancone. 2010. Exosomes/microvesicles as a mechanism of cell-to-cell communication. *Kidney Int.* 78: 838–848.

12. Dellepiane, S., D. Medica, A. D. Quercia, and V. Cantaluppi. 2017. The exciting "bench to bedside" journey of cell therapies for acute kidney injury and renal transplantation. *J. Nephrol.* 30: 319–336.

13. Hunter, M. P., N. Ismail, X. Zhang, B. D. Aguda, E. J. Lee, L. Yu, T. Xiao, J. Schafer, M.-L. T. Lee, T. D. Schmittgen, S. P. Nana-Sinkam, D. Jarjoura, and C. B. Marsh. 2008. Detection of microRNA expression in human peripheral blood microvesicles. *PloS One* 3: e3694.

14. Fleury, A., M. C. Martinez, and S. Le Lay. 2014. Extracellular vesicles as therapeutic tools in cardiovascular diseases. *Front. Immunol.* 5: 370.

15. Revenfeld, A. L. S., R. Bæk, M. H. Nielsen, A. Stensballe, K. Varming, and M. Jørgensen. 2014. Diagnostic and prognostic potential of extracellular vesicles in peripheral blood. *Clin. Ther.*

430 36: 830–846.
431 16. Zhu, H., and G.-C. Fan. 2011. Extracellular/circulating microRNAs and their potential role in
432 cardiovascular disease. *Am. J. Cardiovasc. Dis.* 1: 138–149.
433 17. Fichtlscherer, S., A. M. Zeiher, and S. Dimmeler. 2011. Circulating microRNAs: biomarkers or
434 mediators of cardiovascular diseases? *Arterioscler. Thromb. Vasc. Biol.* 31: 2383–2390.
435 18. Boulanger, C. M., N. Amabile, and A. Tedgui. 2006. Circulating microparticles: a potential
436 prognostic marker for atherosclerotic vascular disease. *Hypertension* 48: 180–186.
437 19. Burton, J. O., H. A. Hamali, R. Singh, N. Abbasian, R. Parsons, A. K. Patel, A. H. Goodall, and
438 N. J. Brunskill. 2013. Elevated levels of procoagulant plasma microvesicles in dialysis patients.
439 *PloS One* 8: e72663.
440 20. Pedrini, L. A., V. De Cristofaro, B. Pagliari, and F. Samà. 2000. Mixed predilution and
441 postdilution online hemodiafiltration compared with the traditional infusion modes. *Kidney Int.* 58:
442 2155–2165.
443 21. Figliolini, F., V. Cantaluppi, M. De Lena, S. Beltramo, R. Romagnoli, M. Salizzoni, R. Melzi,
444 R. Nano, L. Piemonti, C. Tetta, L. Biancone, and G. Camussi. 2014. Isolation, characterization and
445 potential role in beta cell-endothelium cross-talk of extracellular vesicles released from human
446 pancreatic islets. *PloS One* 9: e102521.
447 22. Campean, V., D. Neureiter, B. Nonnast-Daniel, C. Garlichs, M.-L. Gross, and K. Amann. 2007.
448 CD40-CD154 expression in calcified and non-calcified coronary lesions of patients with chronic
449 renal failure. *Atherosclerosis* 190: 156–166.
450 23. Afek, A., D. Harats, A. Roth, G. Keren, and J. George. 2005. A functional role for inducible
451 costimulator (ICOS) in atherosclerosis. *Atherosclerosis* 183: 57–63.
452 24. Migliori, M., V. Cantaluppi, C. Mannari, A. A. E. Bertelli, D. Medica, A. D. Quercia, V.
453 Navarro, A. Scatena, L. Giovannini, L. Biancone, and V. Panichi. 2015. Caffeic Acid, a Phenol
454 Found in White Wine, Modulates Endothelial Nitric Oxide Production and Protects from Oxidative
455 Stress-Associated Endothelial Cell Injury. *PLoS ONE* 10.

456 25. Niwa, T. 2013. Removal of protein-bound uraemic toxins by haemodialysis. *Blood Purif.* 35
457 Suppl 2: 20–25.
458 26. Yamamoto, S., J. J. Kazama, T. Wakamatsu, Y. Takahashi, Y. Kaneko, S. Goto, and I. Narita.
459 2016. Removal of uremic toxins by renal replacement therapies: a review of current progress and
460 future perspectives. *Ren. Replace. Ther.* 2: 43.
461 27. Shroff, R. C., R. McNair, N. Figg, J. N. Skepper, L. Schurgers, A. Gupta, M. Hiorns, A. E.
462 Donald, J. Deanfield, L. Rees, and C. M. Shanahan. 2008. Dialysis accelerates medial vascular
463 calcification in part by triggering smooth muscle cell apoptosis. *Circulation* 118: 1748–1757.
464 28. Jankowski, J., J. Hagemann, M. S. Yoon, M. van der Giet, N. Stephan, W. Zidek, H. Schlüter,
465 and M. Tepel. 2001. Increased vascular growth in hemodialysis patients induced by platelet-derived
466 diadenosine polyphosphates. *Kidney Int.* 59: 1134–1141.
467 29. Chen, X.-D., M. Deng, J.-S. Zhou, Y.-Z. Xiao, X.-S. Zhou, C.-C. Zhang, M. Wu, Z.-D. Wang,
468 and X.-T. Chen. 2015. Bone Morphogenetic Protein-2 regulates in vitro osteogenic differentiation
469 of mouse adipose derived stem cells. *Eur. Rev. Med. Pharmacol. Sci.* 19: 2048–2053.
470 30. Li, S., H. Chen, J. Ren, Q. Geng, J. Song, C. Lee, C. Cao, J. Zhang, and N. Xu. 2014.
471 MicroRNA-223 inhibits tissue factor expression in vascular endothelial cells. *Atherosclerosis* 237:
472 514–520.
473 31. Yigit, I. P., H. Celiker, A. Dogukan, N. Ilhan, A. Gurel, R. Ulu, and B. Aygen. 2015. Can serum
474 NGAL levels be used as an inflammation marker on hemodialysis patients with permanent catheter?
475 *Ren. Fail.* 37: 77–82.
476 32. Cantaluppi, V., S. Dellepiane, M. Tamagnone, D. Medica, F. Figliolini, M. Messina, A. M.
477 Manzione, M. Gai, G. Tognarelli, A. Ranghino, C. Dolla, S. Ferrario, C. Tetta, G. P. Segoloni, G.
478 Camussi, and L. Biancone. 2015. Neutrophil Gelatinase Associated Lipocalin Is an Early and
479 Accurate Biomarker of Graft Function and Tissue Regeneration in Kidney Transplantation from
480 Extended Criteria Donors. *PloS One* 10: e0129279.
481 33. Canaud, B., J. L. Bragg-Gresham, M. R. Marshall, S. Desmeules, B. W. Gillespie, T. Depner, P.

Klassen, and F. K. Port. 2006. Mortality risk for patients receiving hemodiafiltration versus hemodialysis: European results from the DOPPS. *Kidney Int.* 69: 2087–2093.

34. Merello Godino, J. I., R. Rentero, G. Orlandini, D. Marcelli, and C. Ronco. 2002. Results from EuCliD (European Clinical Dialysis Database): impact of shifting treatment modality. *Int. J. Artif. Organs* 25: 1049–1060.

35. Canaud, B., C. Barbieri, D. Marcelli, F. Bellocchio, S. Bowry, F. Mari, C. Amato, and E. Gatti. 2015. Optimal convection volume for improving patient outcomes in an international incident dialysis cohort treated with online hemodiafiltration. *Kidney Int.* 88: 1108–1116.

36. de Sequera, P., M. Albalate, R. Pérez-García, E. Corchete, M. Puerta, M. Ortega, R. Alcázar, T. Talaván, and M. J. Ruiz-Álvarez. 2013. A comparison of the effectiveness of two online haemodiafiltration modalities: mixed versus post-dilution. *Nefrol. Publ. Of. Soc. Esp. Nefrol.* 33: 779–787.

37. Cantaluppi, V., D. Medica, C. Mannari, G. Stiaccini, F. Figliolini, S. Dellepiane, A. D. Quercia, M. Migliori, V. Panichi, L. Giovannini, S. Bruno, C. Tetta, L. Biancone, and G. Camussi. 2015. Endothelial progenitor cell-derived extracellular vesicles protect from complement-mediated mesangial injury in experimental anti-Thy1.1 glomerulonephritis. *Nephrol. Dial. Transplant. Off. Publ. Eur. Dial. Transpl. Assoc. - Eur. Ren. Assoc.* 30: 410–422.

38. Clement, M., K. Guedj, F. Andreata, M. Morvan, L. Bey, J. Khallou-Laschet, A.-T. Gaston, S. Delbosc, J.-M. Alsac, P. Bruneval, C. Deschildre, M. Le Borgne, Y. Castier, H.-J. Kim, H. Cantor, J.-B. Michel, G. Caligiuri, and A. Nicoletti. 2015. Control of the T follicular helper-germinal center B-cell axis by $CD8^+$ regulatory T cells limits atherosclerosis and tertiary lymphoid organ development. *Circulation* 131: 560–570.

39. Packard, R. R. S., and P. Libby. 2008. Inflammation in atherosclerosis: from vascular biology to biomarker discovery and risk prediction. *Clin. Chem.* 54: 24–38.

40. Gerdes, N., and A. Zirlik. 2011. Co-stimulatory molecules in and beyond co-stimulation - tipping the balance in atherosclerosis? *Thromb. Haemost.* 106: 804–813.

508 41. Desideri, G., V. Panichi, S. Paoletti, D. Grassi, R. Bigazzi, S. Beati, G. Bernabini, A. Rosati, C.
509 Ferri, S. Taddei, L. Ghiadoni, and RISCAVID investigators. 2011. Soluble CD40 ligand is
510 predictive of combined cardiovascular morbidity and mortality in patients on haemodialysis at a
511 relatively short-term follow-up. *Nephrol. Dial. Transplant. Off. Publ. Eur. Dial. Transpl. Assoc. -*
512 *Eur. Ren. Assoc.* 26: 2983–2988.
513 42. Cantaluppi, V., A. D. Quercia, S. Dellepiane, S. Ferrario, G. Camussi, and L. Biancone. 2014.
514 Interaction between systemic inflammation and renal tubular epithelial cells. *Nephrol. Dial.*
515 *Transplant. Off. Publ. Eur. Dial. Transpl. Assoc. - Eur. Ren. Assoc.* 29: 2004–2011.
516 43. Dellepiane, S., M. Marengo, and V. Cantaluppi. 2016. Detrimental cross-talk between sepsis
517 and acute kidney injury: new pathogenic mechanisms, early biomarkers and targeted therapies. *Crit.*
518 *Care Lond. Engl.* 20: 61.
519 44. Taïbi, F., V. Metzinger-Le Meuth, E. M'Baya-Moutoula, M. seif el I. Djelouat, L. Louvet, J.-M.
520 Bugnicourt, S. Poirot, A. Bengrine, J.-M. Chillon, Z. A. Massy, and L. Metzinger. 2014. Possible
521 involvement of microRNAs in vascular damage in experimental chronic kidney disease. *Biochim.*
522 *Biophys. Acta* 1842: 88–98.
523 45. Taïbi, F., V. Metzinger-Le Meuth, Z. A. Massy, and L. Metzinger. 2014. miR-223: An
524 inflammatory oncomiR enters the cardiovascular field. *Biochim. Biophys. Acta* 1842: 1001–1009.
525 46. Wang, Y., Y. Zhang, J. Huang, X. Chen, X. Gu, Y. Wang, L. Zeng, and G.-Y. Yang. 2014.
526 Increase of circulating miR-223 and insulin-like growth factor-1 is associated with the pathogenesis
527 of acute ischemic stroke in patients. *BMC Neurol.* 14: 77.
528 47. Dai, G.-H., P.-Z. Ma, X.-B. Song, N. Liu, T. Zhang, and B. Wu. 2014. MicroRNA-223-3p
529 inhibits the angiogenesis of ischemic cardiac microvascular endothelial cells via affecting
530 RPS6KB1/hif-1a signal pathway. *PloS One* 9: e108468.
531 48. Wang, Y.-S., J. Zhou, K. Hong, X.-S. Cheng, and Y.-G. Li. 2015. MicroRNA-223 displays a
532 protective role against cardiomyocyte hypertrophy by targeting cardiac troponin I-interacting
533 kinase. *Cell. Physiol. Biochem. Int. J. Exp. Cell. Physiol. Biochem. Pharmacol.* 35: 1546–1556.

534 49. Shrestha, K., A. G. Borowski, R. W. Troughton, A. L. Klein, and W. H. W. Tang. 2012.
535 Association between systemic neutrophil gelatinase-associated lipocalin and anemia, relative
536 hypochromia, and inflammation in chronic systolic heart failure. *Congest. Heart Fail. Greenwich*
537 *Conn* 18: 239–244.
538 50. Rangrez, A. Y., E. M'Baya-Moutoula, V. Metzinger-Le Meuth, L. Hénaut, M. S. el I. Djelouat,
539 J. Benchitrit, Z. A. Massy, and L. Metzinger. 2012. Inorganic phosphate accelerates the migration
540 of vascular smooth muscle cells: evidence for the involvement of miR-223. *PloS One* 7: e47807.
541 51. M'Baya-Moutoula, E., L. Louvet, V. Metzinger-Le Meuth, Z. A. Massy, and L. Metzinger.
542 2015. High inorganic phosphate concentration inhibits osteoclastogenesis by modulating miR-223.
543 *Biochim. Biophys. Acta* 1852: 2202–2212.
544
545

FIGURE LEGENDS

Figure 1: Study flow chart

Figure 2: Clinical and intradialytic parameters: Trend lines demonstrate the values of (A) β2-microglobulin, (B) C-reactive protein - CRP, (C) IL6, (D) serum iron, (E) transferrin saturation, (F) ferritin, (G) Neutrophil Gelatinase Associated Lipocalin - NGAL, (H) hemoglobin and (I) erythropoiesis resistance index - ERI across the study time points. *: $p<0.05$ vs. T0, BHD: standard bicarbonate hemodialysis, mOL-HDF: mixed on-line hemodiafiltration, T0: study start, T1, 2 and 3: 3, 6 and 9 months of treatment start.

Figure 3: Nanosight and western blot analysis of plasma extracellular vesicles (EV). (A) Plasma extracellular vesicles (EV) concentration at the different study time points in patients randomized to BHD (n=15) or mOL-HDF (n=15) and in a group of healthy subjects (only T0). (B) Representative Nanosight Tracking Analysis plots and medium EV size for each healthy subject, BHD and mOL-HDF patient enrolled. (C) Representative WB analysis of CD9, CD63 and β-actin protein content in healthy-, BHD- and mOL-HDF-EV. (D) EV Quantification in the control cohort of healthy subjects (n=10), stage IV CKD (n=20), peritoneal dialysis (PD) (n=10), BHD hemodialysis (n=50) or post-dilution OL-HDF patients (n=30). Hemodialysis patients were subdivided according to vascular access type (arteriovenous fistula - AVF, n=57; central venous catheter - CVC, n=23). Statistical analysis was performed by ANOVA with Newman-Keuls multicomparison test. *: $p<0.05$ vs. healthy, BHD: standard bicarbonate hemodialysis, (m)OL-HDF: (mixed) on-line hemodiafiltration, T0: study start, T1, 2 and 3: 3, 6 and 9 months of treatment start.

Figure 4: Guava FACS analysis of plasma extracellular vesicles (EV). (A) Histograms showing the positivity rate (%) for exosome, platelet, monocyte/macrophage, T-cell, B-cell and endothelial cell markers, (see Material and Methods) in EV derived from healthy subjects, BHD or mOL-HDF patients at study start. *: $p < 0.05$ vs. healthy. (B) Histograms showing the positivity rate (%) for

marker of uremia related atherosclerosis and inflammation in EV derived from healthy subjects, BHD or mOL-HDF patients at study start. (C) Quantification of endothelial-derived EV in the control cohort of healthy subjects (n=10), stage IV CKD (n=20), peritoneal dialysis (PD) (n=10), BHD hemodialysis (n=50) or post-dilution OL-HDF patients (n=30). Hemodialysis patients were subdivided according to vascular access type (arteriovenous fistula - AVF, n=57; central venous catheter - CVC, n=23). Statistical analysis was performed by ANOVA with Newman-Keuls multicomparison test. *: $p<0.05$ vs. healthy, BHD: standard bicarbonate hemodialysis, (m)OL-HDF: (mixed) on-line hemodiafiltration, T0: study start, T1, 2 and 3: 3, 6 and 9 months of treatment start.

Figure 5: Analysis of microRNA content in plasma extracellular vesicles (EV) of hemodialysis patients. (A) Protein Quest web-based analysis identified 5 different miRNAs (miR-17a-5p, miR-92a, miR-223, miR-423-5p, miR-451) involved in endothelial dysfunction and vascular calcification. Squares represent miRNAs, whereas circles represent proteins. Node dimension correlates with literature frequency of displayed molecules; line thickness represents the number of literature co-occurrence between elements. (B-F) Relative quantification by real-time PCR (RT-PCR) for EV expression of the 5 identified miRNAs in healthy controls, BHD- and mOL-HDF patients at the different study time points. (G) qRT-PCR for miR-223 in in the control cohort of healthy subjects (n=10), stage IV CKD (n=20), peritoneal dialysis (PD) (n=10), BHD hemodialysis (n=50) or post-dilution OL-HDF patients (n=30). Hemodialysis patients were subdivided according to vascular access type (arteriovenous fistula - AVF, n=57; central venous catheter - CVC, n=23). Statistical analysis was performed by ANOVA with Newman-Keuls multicomparison test. *: $p<0.05$ vs. healthy, §: $p<0.05$ vs. BHD, BHD: standard bicarbonate hemodialysis, (m)OL-HDF: (mixed) on-line hemodiafiltration, T0: study start, T1, 2 and 3: 3, 6 and 9 months of treatment start.

Figure 6: Effect of plasma extracellular vesicles (EV) on *in vitro* endothelial angiogenesis and apoptosis. (A) Histogram showing the quantitative analysis of the *in vitro* HUVEC angiogenesis assay after different stimuli; *: $p<0.05$ vs. CTRL, §: $p< 0.05$ vs. BHD-EV (B) Histogram showing

the quantitative analysis of the *in vitro* TUNEL apoptosis assay on HUVEC subjected to different stimuli; *: $p<0.05$ vs. CTRL, §: $p< 0.05$ vs. BHD-EV. (C) Quantitative analysis of angiogenesis assay in HUVEC transfected with miR-223 mimic or inhibitor and stimulated with patients EV; *: $p<0.05$ vs. CTRL (D) Quantitative analysis of HUVEC angiogenesis assay after stimulation with patients EV transfected or not with miR-223-inhibitor; *: $p<0.05$ vs. BHD EV. BHD: bicarbonate hemodialysis, CTRL: control group, HUVEC: human umbilical vascular endothelial cells, mOL-HDF: mixed online hemodiafiltration, Uremic Toxins: ADMA 10 μg/ml + p-cresyl sulphate 1 μg/ml and indoxyl sulphate 10 μg/ml, VEGF: vascular endothelial growth factor.

Figure 7: Role of plasma extracellular vesicle (EV)-carried miR-223 in osteoblastic differentiation of vascular smooth muscle cells (VSMC). (A) Representative images and (B) relative quantification of red alizarin staining of VSMC incubated with EV derived from healthy subjects, BHD or mOL-HDF patients; *: $p< 0.05$ vs. healthy EV, §: $p < 0.05$ vs. BHD EV. (C) Quantitative real time PCR for RUNX2 mRNA expression in VSMC incubated with EV derived from healthy subjects, BHD or mOL-HDF patients; *: $p< 0.05$ vs. healthy EV, §: $p < 0.05$ vs. BHD EV. (D) Quantitative analysis of red alizarin staining in VSMC transfected with miR-223 mimic or inhibitor and stimulated with patients EV; *: $p<0.05$ vs. CTRL, §: $p<0.05$ vs. mimic. (D) Quantitative analysis of VSMC staining after stimulation with patients EV transfected or not with miR-223-inhibitor; *: $p<0.05$ vs. BHD EV. BHD: bicarbonate hemodialysis, CTRL: control group, mOL-HDF: mixed online hemodiafiltration.

Figure 8: Analysis of miR-223 target genes: role of IGF1R. (A) Ingenuity IPA pathway analysis predicted target genes for miR-223. Pointed arrowheads represent activating relationships whereas solid or dotted edges indicate direct or indirect relationships, respectively. Relationship between miR-223 and IGF1R is highlighted. (B) Representative WB analysis and (C) relative quantification of IGF1R protein expression in HUVEC after stimulation with healthy, BHD or mOL-HDF patient EV or after transfection with miR-223 mimic or after stimulation with BHD patient EV transfected with miR-223 inhibitor. *: $p < 0.05$ vs. healthy §: $p < 0.05$ mimic-223 vs. BHD. BHD: bicarbonate

hemodialysis, CTRL: control group, EV: extracellular vesicles, IGF1R: insulin like growth factor 1 receptor, mOL-HDF: mixed online hemodiafiltration.

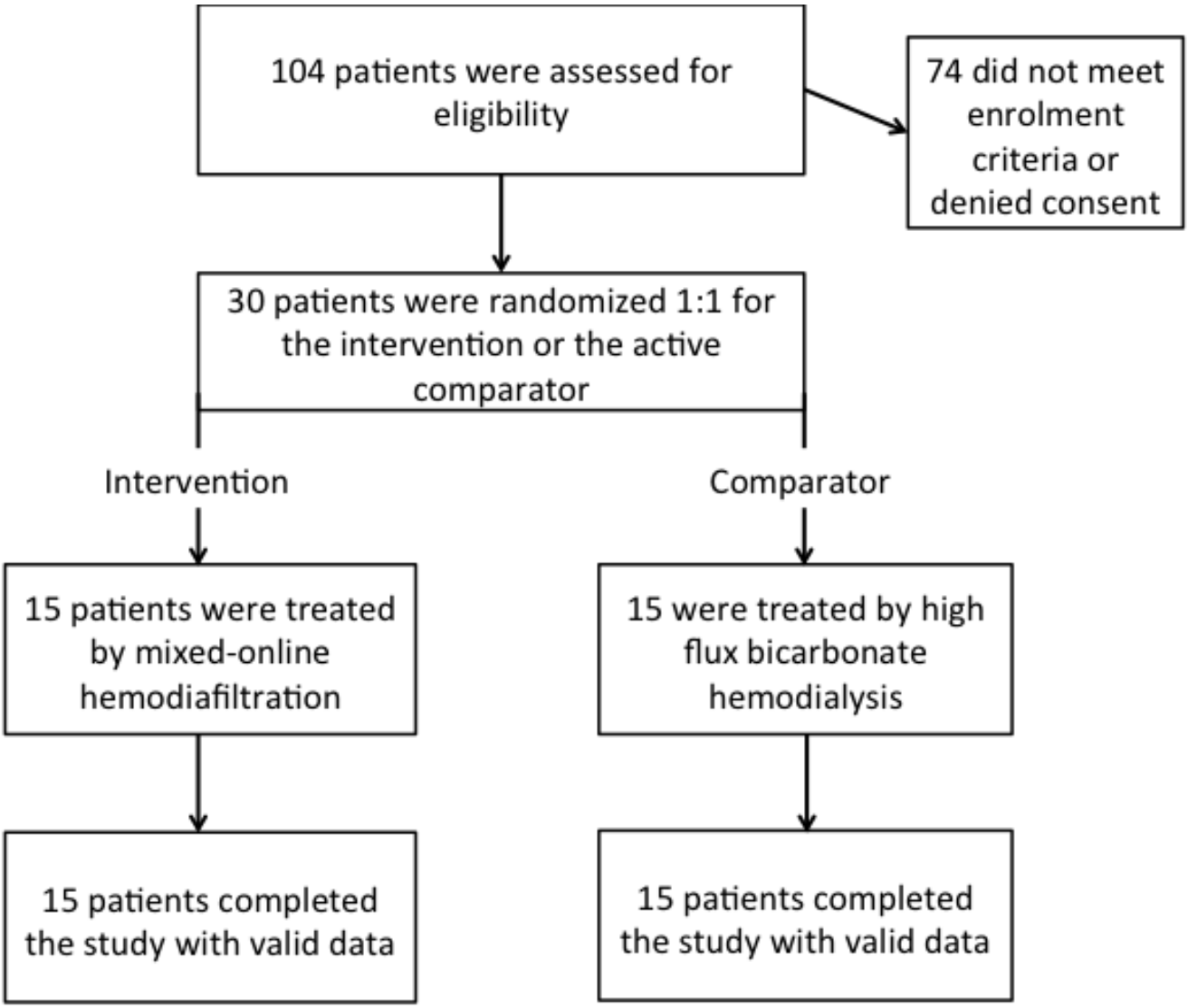
104 patients were assessed for eligibility
74 did not meet enrolment criteria or denied consent
30 patients were randomized 1:1 for the intervention or the active comparator
Intervention
Comparator
15 patients were treated by mixed-online hemodiafiltration
15 were treated by high flux bicarbonate hemodialysis
15 patients completed the study with valid data
15 patients completed the study with valid data

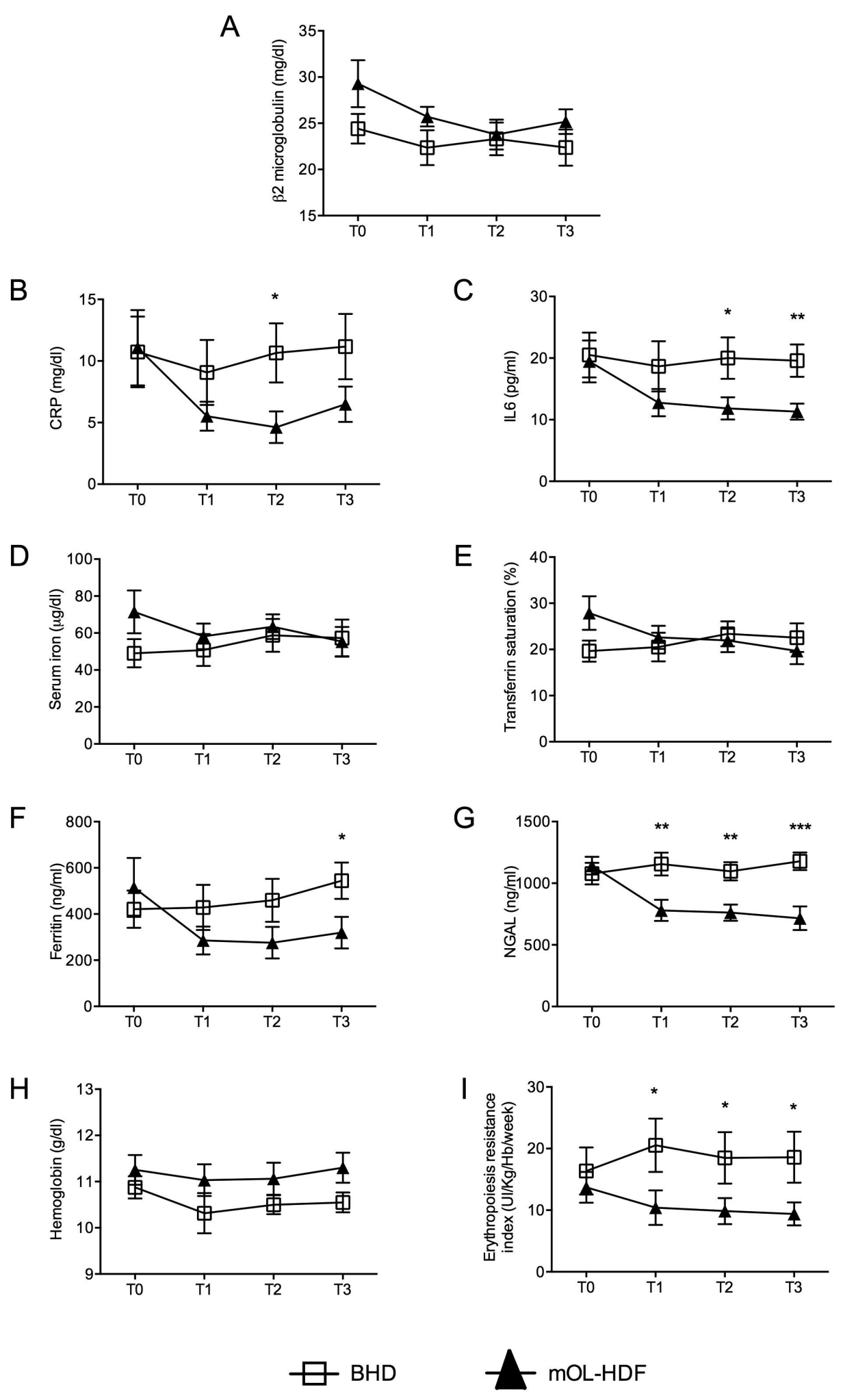
A
β2 microglobulin (mg/dl)
35
30
25
20
15
T0
T1
T2
T3
B
CRP (mg/dl)
15
10
5
0
*
T0
T1
T2
T3
C
IL6 (pg/ml)
30
20
10
0
*
**
T0
T1
T2
T3
D
Serum iron (µg/dl)
100
80
60
40
20
0
T0
T1
T2
T3
E
Transferrin saturation (%)
40
30
20
10
0
T0
T1
T2
T3
F
Ferritin (ng/ml)
800
600
400
200
0
*
T0
T1
T2
T3
G
NGAL (ng/ml)
1500
1000
500
0
**
**
***
T0
T1
T2
T3
H
Hemoglobin (g/dl)
13
12
11
10
9
T0
T1
T2
T3
I
Erythropoiesis resistance index (UI/Kg/Hb/week)
30
20
10
0
*
*
*
T0
T1
T2
T3
BHD
mOL-HDF

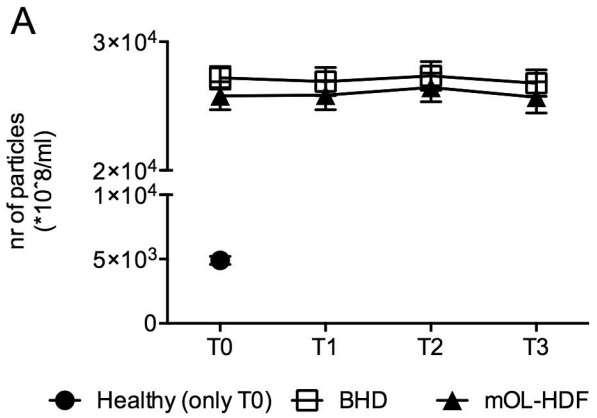
A
3×10^4
2×10^4
1×10^4
5×10^3
0
nr of particles (*10^8/ml)
T0
T1
T2
T3
Healthy (only T0)
BHD
mOL-HDF

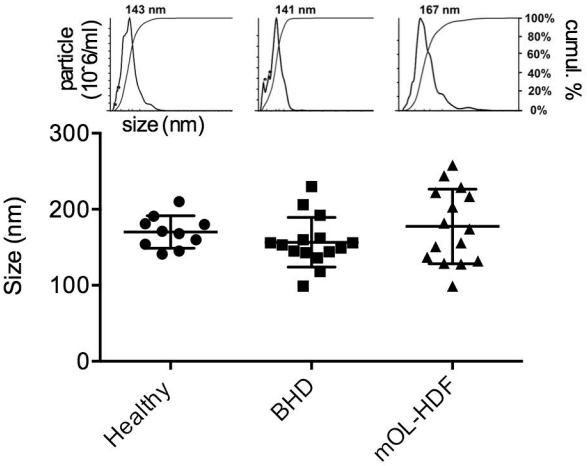
B
143 nm
141 nm
167 nm
particle (10^6/ml)
cumul. %
100%
80%
60%
40%
20%
0%
size (nm)
300
200
100
0
Size (nm)
Healthy
BHD
mOL-HDF

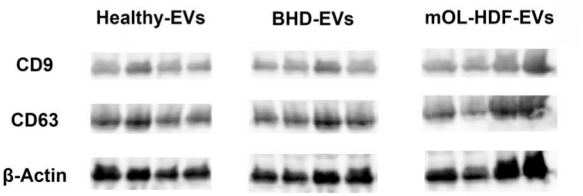
C
Healthy-EVs
BHD-EVs
mOL-HDF-EVs
CD9
CD63
β-Actin

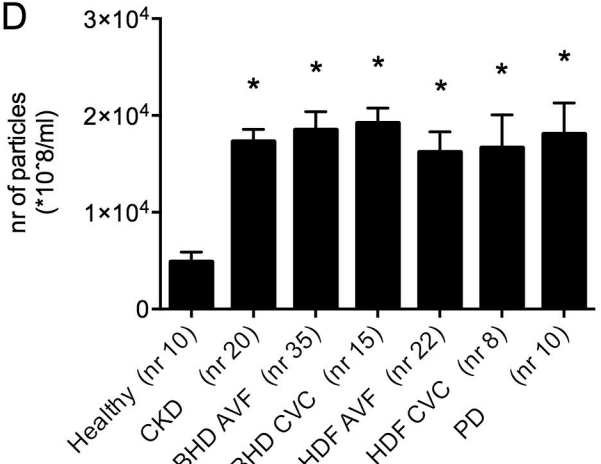
D
3×10^4
2×10^4
1×10^4
0
nr of particles (*10^8/ml)
*
Healthy (nr 10)
CKD (nr 20)
BHD AVF (nr 35)
BHD CVC (nr 15)
HDF AVF (nr 22)
HDF CVC (nr 8)
PD (nr 10)

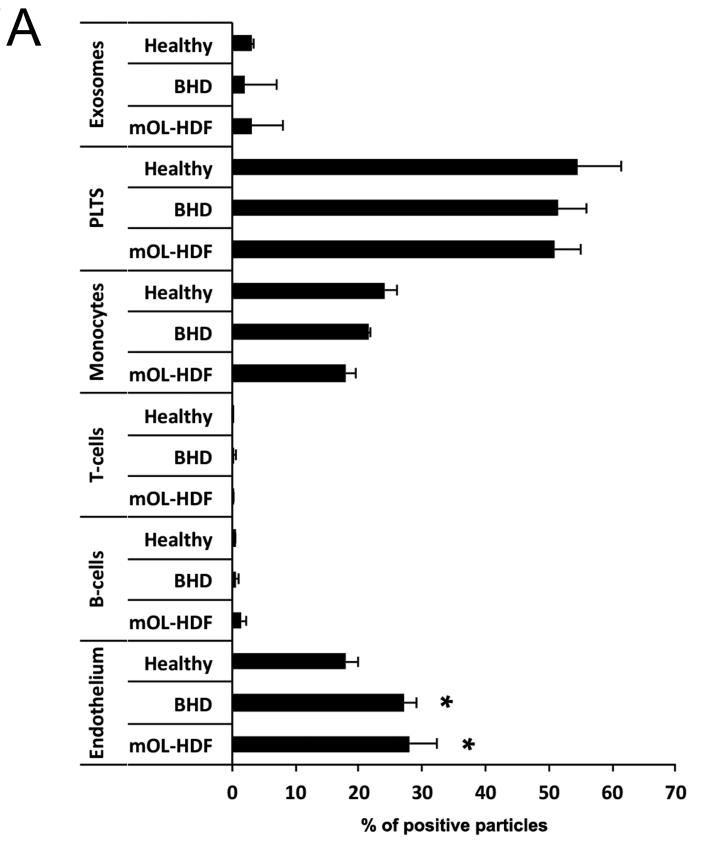
A
Exosomes
PLTS
Monocytes
T-cells
B-cells
Endothelium
Healthy
BHD
mOL-HDF
*
0
10
20
30
40
50
60
70
% of positive particles

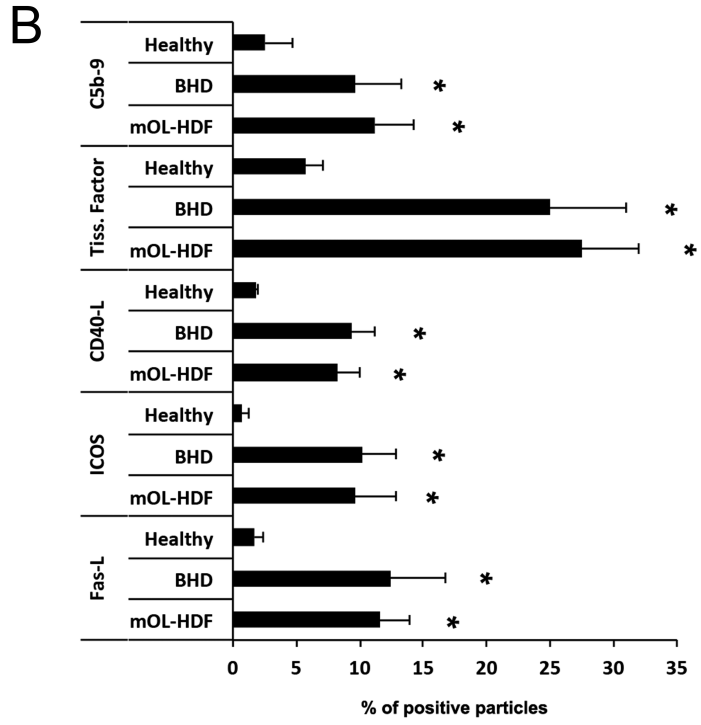
B
C5b-9
Tiss. Factor
CD40-L
ICOS
Fas-L
Healthy
BHD
mOL-HDF
*
0
5
10
15
20
25
30
35
% of positive particles

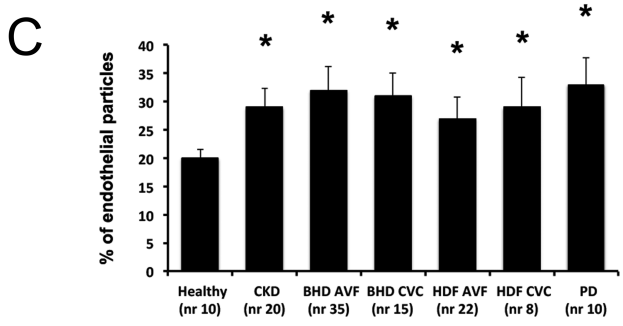
C
% of endothelial particles
*
0
5
10
15
20
25
30
35
40
Healthy (nr 10)
CKD (nr 20)
BHD AVF (nr 35)
BHD CVC (nr 15)
HDF AVF (nr 22)
HDF CVC (nr 8)
PD (nr 10)

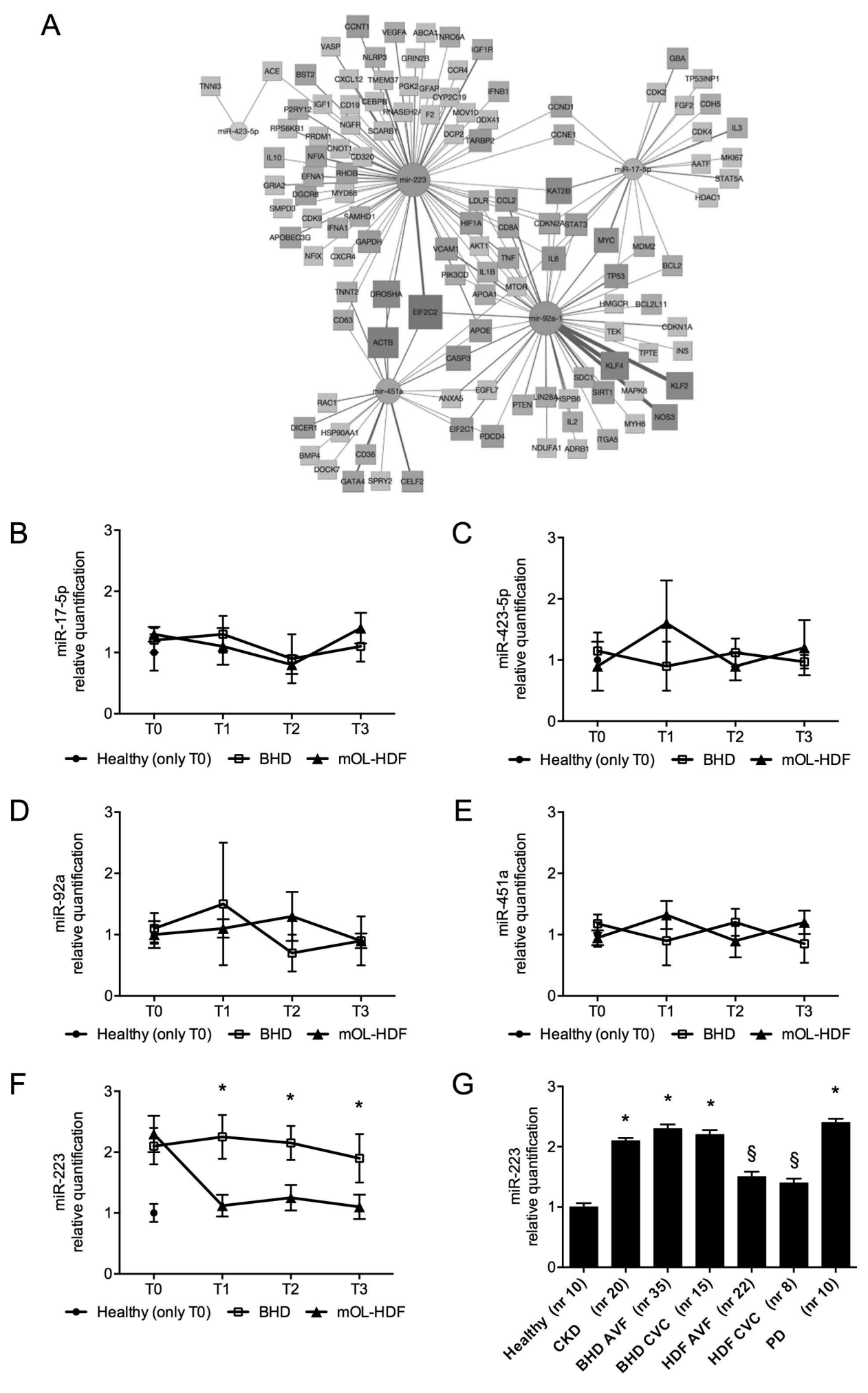
A
miR-423-5p
mir-223
miR-17-5p
mir-92a-1
mir-451a
B
miR-17-5p
relative quantification
C
miR-423-5p
relative quantification
D
miR-92a
relative quantification
E
miR-451a
relative quantification
F
miR-223
relative quantification
G
miR-223
relative quantification
T0
T1
T2
T3
Healthy (only T0)
BHD
mOL-HDF
Healthy (nr 10)
CKD (nr 20)
BHD AVF (nr 35)
BHD CVC (nr 15)
HDF AVF (nr 22)
HDF CVC (nr 8)
PD (nr 10)

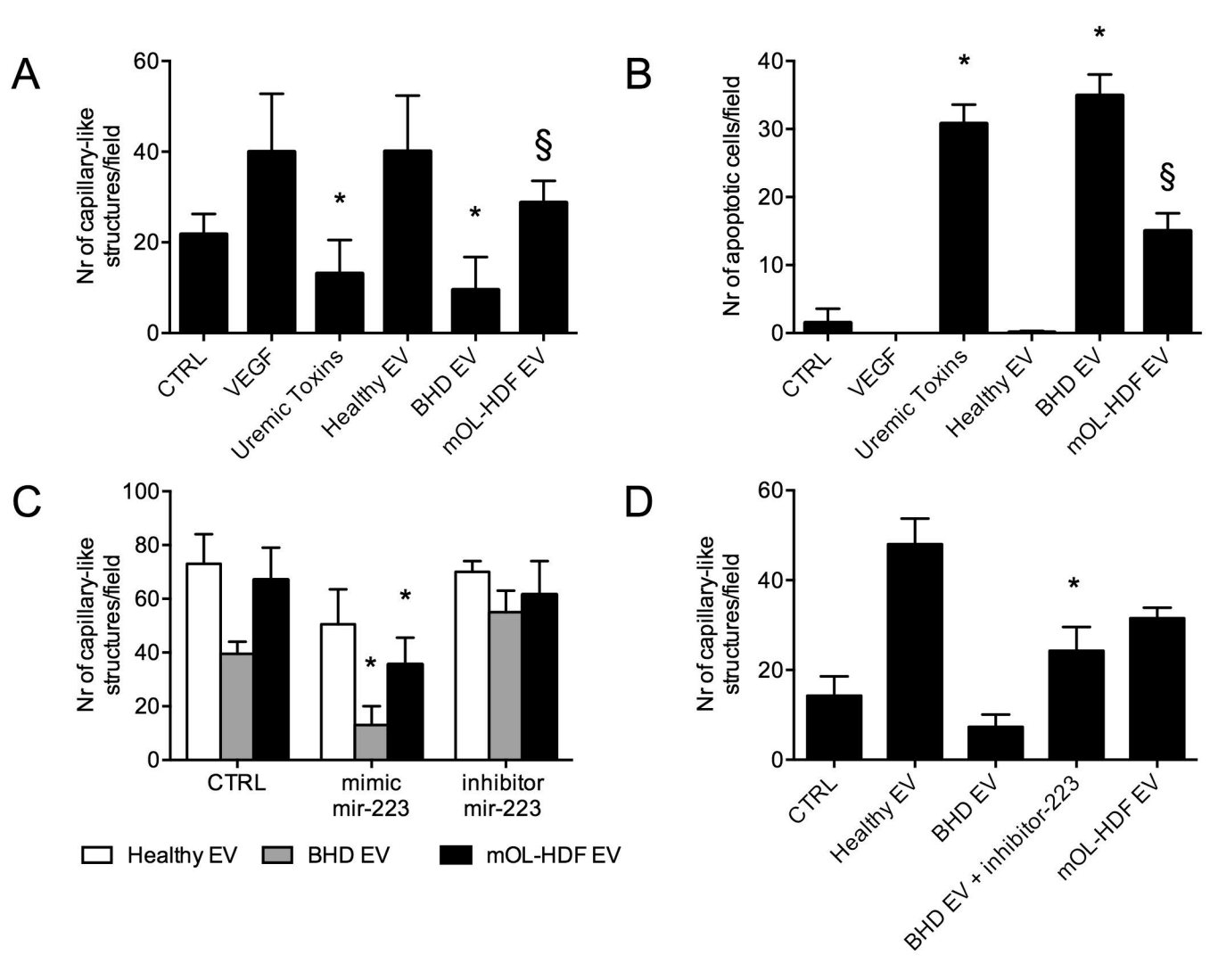
A
Nr of capillary-like structures/field
60
40
20
0
*
*
§
CTRL
VEGF
Uremic Toxins
Healthy EV
BHD EV
mOL-HDF EV
B
Nr of apoptotic cells/field
40
30
20
10
0
*
*
§
CTRL
VEGF
Uremic Toxins
Healthy EV
BHD EV
mOL-HDF EV
C
Nr of capillary-like structures/field
100
80
60
40
20
0
*
*
CTRL
mimic mir-223
inhibitor mir-223
Healthy EV
BHD EV
mOL-HDF EV
D
Nr of capillary-like structures/field
60
40
20
0
*
CTRL
Healthy EV
BHD EV
BHD EV + inhibitor-223
mOL-HDF EV

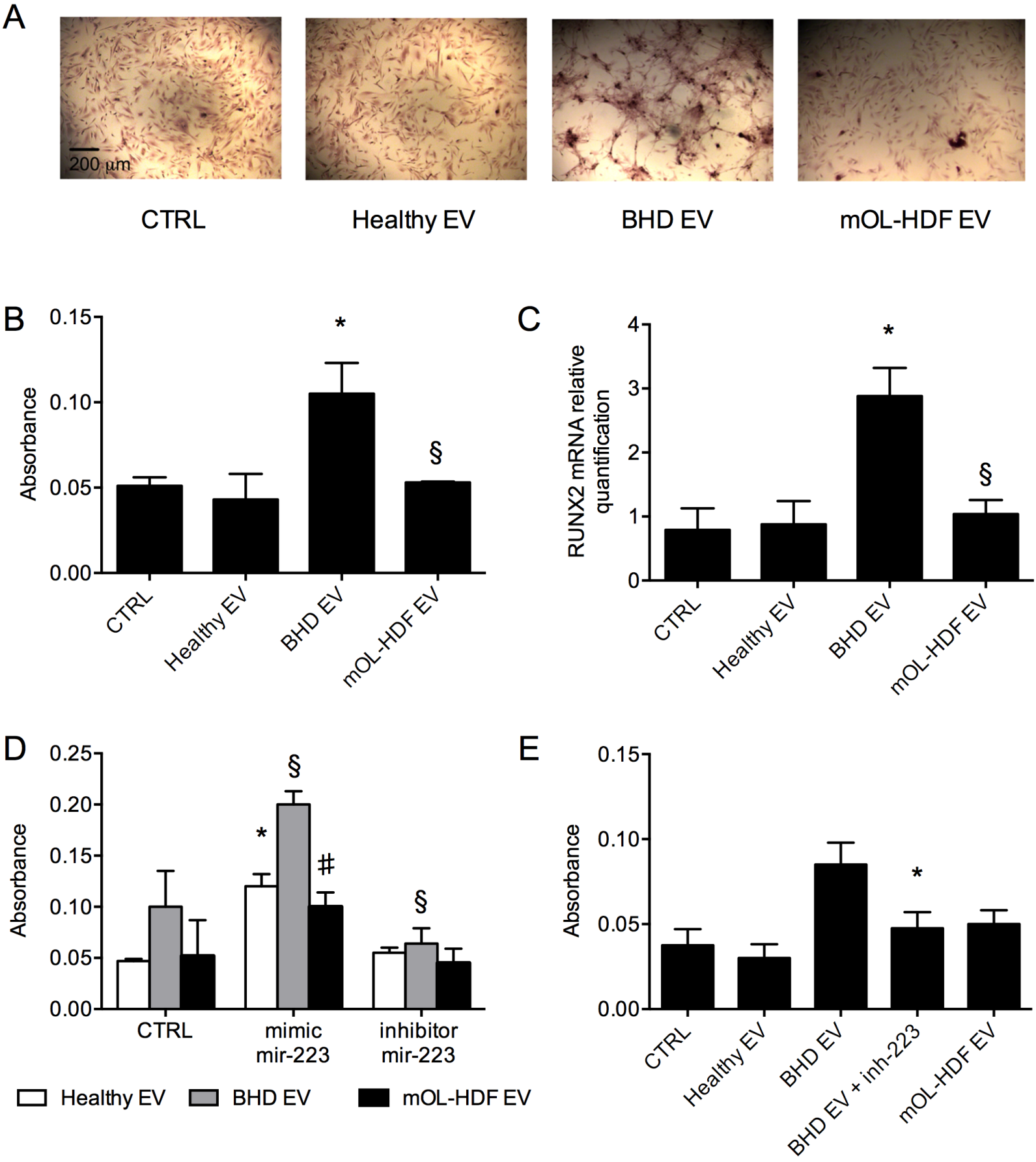
A
200 µm
CTRL
Healthy EV
BHD EV
mOL-HDF EV
B
Absorbance
0.15
0.10
0.05
0.00
*
§
CTRL
Healthy EV
BHD EV
mOL-HDF EV
C
RUNX2 mRNA relative quantification
4
3
2
1
0
*
§
CTRL
Healthy EV
BHD EV
mOL-HDF EV
D
Absorbance
0.25
0.20
0.15
0.10
0.05
0.00
*
§
#
§
CTRL
mimic mir-223
inhibitor mir-223
Healthy EV
BHD EV
mOL-HDF EV
E
Absorbance
0.15
0.10
0.05
0.00
*
CTRL
Healthy EV
BHD EV
BHD EV + inh-223
mOL-HDF EV

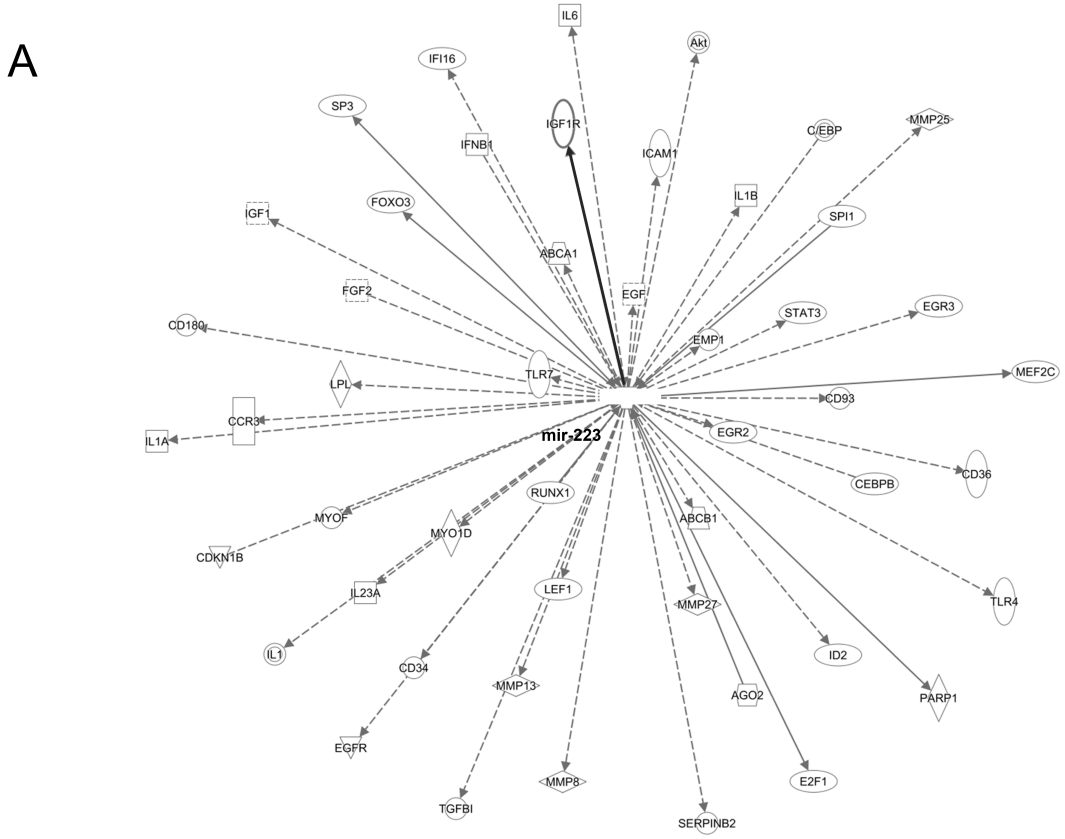
A
IL6
Akt
IFI16
SP3
IGF1R
C/EBP
MMP25
IFNB1
ICAM1
IL1B
FOXO3
SPI1
IGF1
ABCA1
FGF2
EGF
STAT3
EGR3
CD180
EMP1
TLR7
MEF2C
LPL
CD93
CCR3
mir-223
EGR2
IL1A
CEBPB
CD36
RUNX1
MYOF
ABCB1
MYO1D
CDKN1B
LEF1
IL23A
MMP27
TLR4
IL1
ID2
CD34
MMP13
AGO2
PARP1
EGFR
E2F1
MMP8
TGFBI
SERPINB2

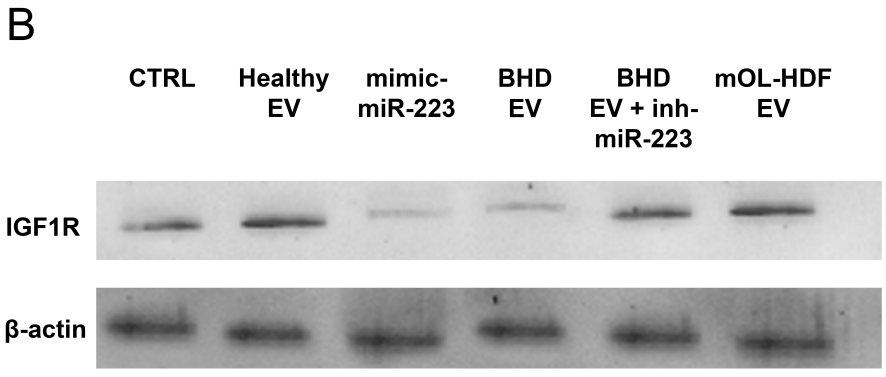
B
CTRL
Healthy EV
mimic-miR-223
BHD EV
BHD EV + inh-miR-223
mOL-HDF EV
IGF1R
β-actin

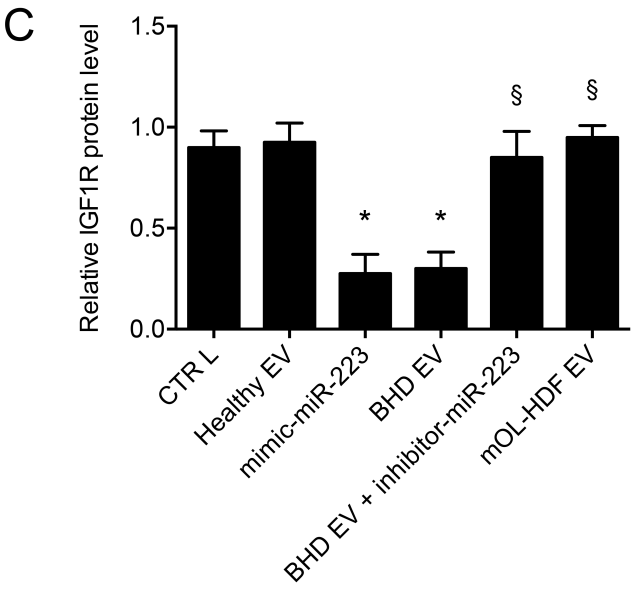
C
Relative IGF1R protein level
1.5
1.0
0.5
0.0
*
*
§
§
CTR L
Healthy EV
mimic-miR-223
BHD EV
BHD EV + inhibitor-miR-223
mOL-HDF EV

	mOL-HDF	BHD	*p*
	Patients' Characteristics		
Gender (female)	23%	33%	0,2
Age	63,75±11	65,5±16,1	0,92
Hypertension	92%	83%	0,49
Diabetes	31%	25%	0,47
CV disease	31%	58%	0,16
Dialysis age (months)	84±75	82±112	0,93
AVF	92%	83%	0,5

Table I: Demographic characteristics, co-morbidities, dialysis age and access type of enrolled patients. AVF: arteriovenous fistula; BHD: bicarbonate Hemodialysis; CV: cardiovascular; mOL-HDF: mixed on-line hemodiafiltration.

	T0		T1		T2		T3		P (ANOVA or χ^2)		
	mOL-HDF*	**BHD**	**mOL-HDF**	**BHD**	**mOL-HDF**	**BHD**	**mOL-HDF**	**BHD**	**Within mOL-HDF**	**Within BHD**	**All**
nPCR	1,12±0,14	1,08±0,12	1,16±0,2	1,1±0,15	1,18±0,2	1,2±0,12	1,15±0,1	1,1±0,18	0,92	0,89	0,88
sPhosphate (mmol/l)	1,44±0,6	1,42±0,2	1,48±0,3	1,41±0,2	1,42±0,3	1,38±0,2	1,41±0,4	1,44±0,2	0,97	0,95	0,99
sCalcium (mmol/l)	2,38±0,2	2,36±0,3	2,36±0,2	2,37±0,2	2,40±0,3	2,33±0,4	2,39±0,3	2,38±0,2	0,82	0,79	0,74
sPTH (pg/ml)	289±205	234±156	229±167	267±172	248±164	221±188	230±127	256±201	0,43	0,36	0,28
Number of HT drugs	1,6±1,2	1,42±1,1	1,5±1,1	1,42±1,1	1,6±1,2	1,5±1,2	1,6±1,2	1,42±1,1	0,97	0,94	0,88
Iv. Iron (mg/week)	37±56	35±22	39±51	31±24	42±56	36±24	50±39	41±21	0,82	0,76	0,88
Statin use	15%	33%	38%	33%	46%	33%	46%	33%	0,31	1	0,41
RAAS blocker	23%	15%	31%	15%	31%	25%	31%	25%	0,82	0,84	0,76
Vitamin D use	100%	100%	100%	92%	100%	92%	100%	92%	1	0,92	0,88
Pre-HD PA≤140/90	69%	75%	69%	66%	84%	75%	84%	66%	0,76	0,65	0,82

Table II: Patients'clinical variables at all considered time-points. BHD: bicarbonate Hemodialysis; HT: hypotensive; Iv: intravenous; mOL-HDF: mixed on-line hemodiafiltration; nPCR: normalized protein catabolic rate; RASS: renin-angiotensin-aldosterone system. *At T0, mOL-HDF group was still treated by BHD. Statistical analysis was performed by one way ANOVA or χ^2 test when appropriated: $p<0.05$ was considered statistically significant.

	T0		T1		T2		T3		P (ANOVA or χ^2)		
	mOL-HDF*	**BHD**	**mOL-HDF**	**BHD**	**mOL-HDF**	**BHD**	**mOL-HDF**	**BHD**	**Within mOL-HDF**	**Within BHD**	**All**
Dialyzer Surface (m^2)	2±15	2,0±0,2	2±15	2,0±0,2	2±15	2,0±0,2	2±15	2,0±0,2	1	1	0,92
Heparin start dose (IU)	1250±210	1458±486	1250±210	1458±486	1250±210	1458±486	1250±210	1458±486	1	1	0,31
Heparin maintenance dose (IU/h)	307±166	333±144	307±166	312±136	307±166	312±136	307±166	333±144	1	0,91	0,68
HD duration (min)	237±8	240±0	237±8	240±0	237±8	240±0	237±8	240±0	1	1	0,63
Qb (ml/min)	317±15	315±18	320±13	322±21	318±14	313±16	319±15	324±26	0,96	0,76	0,65
Qd (ml/min)	500±0	500±0	468±66	500±0	459±67	500±0	466±71	500±0	0,88	1	0,08
TMP (mmHg)	114±13	115±18	268±12	118±12	265±11	112±10	265±12	108±8	0,99	0,56	**<0,01**
Convective Volume (L)	NA	NA	35,1±4,6	NA	33,8±4	NA	34,5±4,2	NA	0,92	NA	NA
Net UF (L)	2,88±0,52	2,75±0,47	2,76±0,54	2,92±0,58	2,85±0,49	3±0,64	2,84±0,43	2,76±0,5	0,78	0,47	0,65
eKt/V	1,34±0,23	1,38±0,24	1,48±0,27	1,36±0,24	1,68±0,34	1,37±0,26	1,48±0,28	1,38±0,22	**0,04**	0,98	**0,03**

Table III: Intradialytic variables at all considered time-points. BHD: bicarbonate Hemodialysis; HD: hemodialysis; mOL-HDF: mixed on-line hemodiafiltration; Qb: blood flow; Qd: dialisys solution flow; TMP: transmembane pressure. *At T0, mOL-HDF group was still treated by BHD. Statistical analysis was performed by one way ANOVA or χ^2 test when appropriated: $p<0.05$ was considered statistically significant.

Supplementary Figures

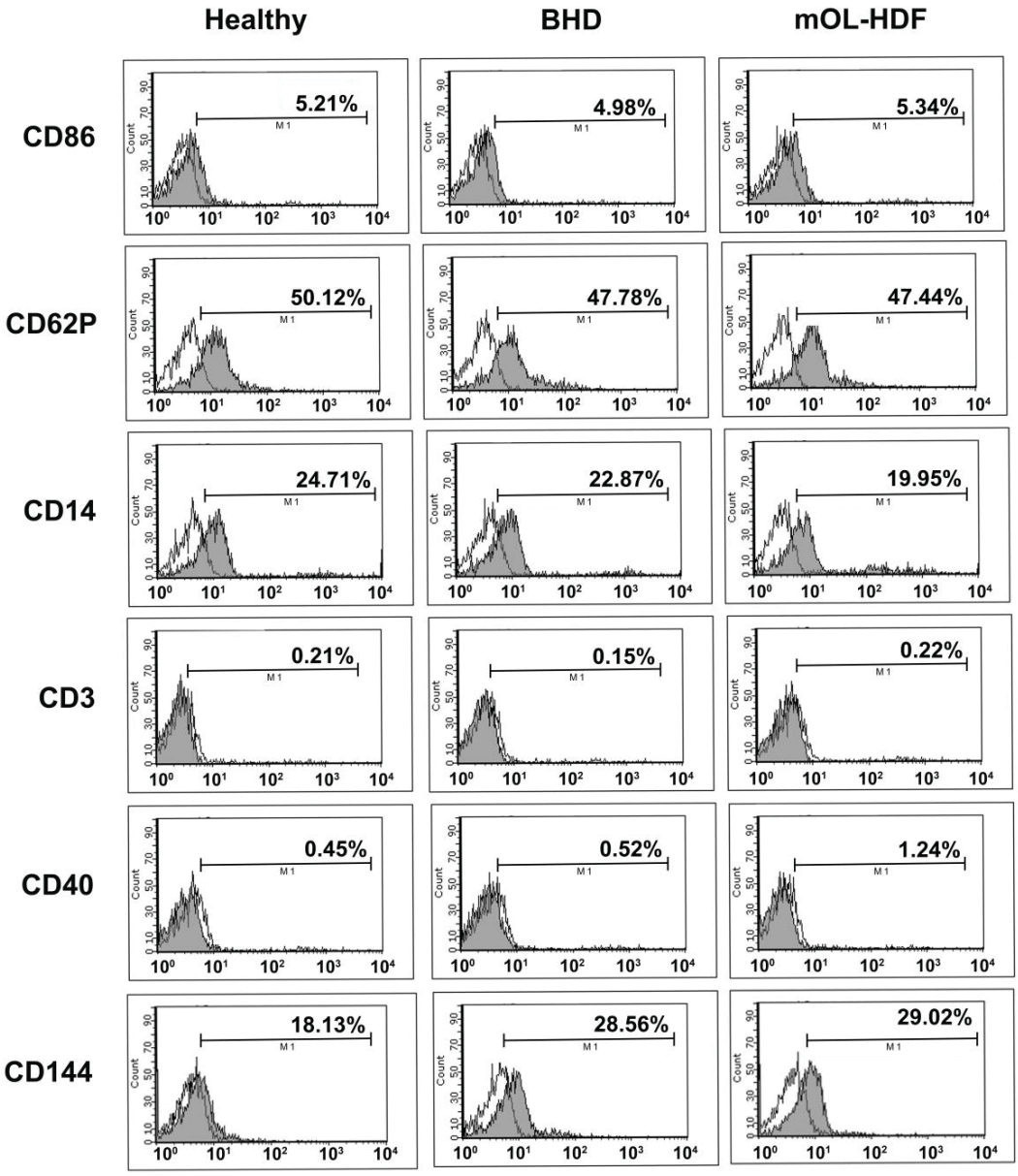

Supplementary figure 1: representative healthy, BHD- and mOL-HDF-EV FACS Guava analysis of the main markers for exosomes (CD86), platelets (CD62P), monocytes/macrophages (CD14), T-cells (CD3), B-cells (CD40) and endothelial cells (CD144). Staining with the different antibodies (gray-filled curves) was compared to internal control (bright-line curve) represented by appropriate secondary isotype incubation

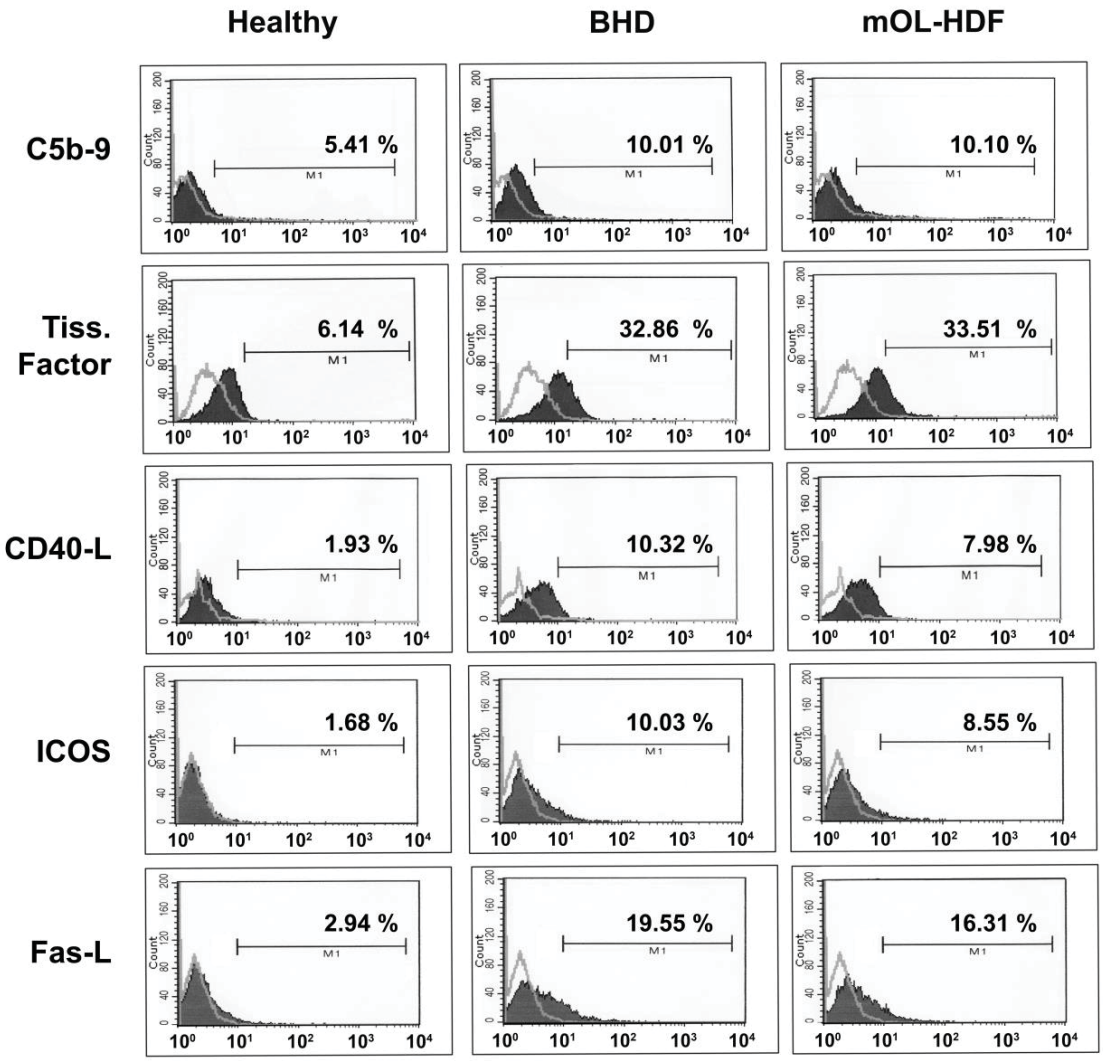

Supplementary figure 2: representative healthy, BHD- and mOL-HDF-EV FACS Guava analysis of molecules involved in inflammation, atherosclerosis, complement and coagulation activation: Membrane Attack Complex/ Terminal Complement Complex (C5b-9), Tissue Factor (Tiss. Factor), CD40-Ligand (CD40-L), Inducible T-cell COStimulator (ICOS), and Fas-Ligand (Fas-L). Staining with the different antibodies (gray-filled curves) was compared to internal control (bright-line curve) represented by appropriate secondary isotype incubation

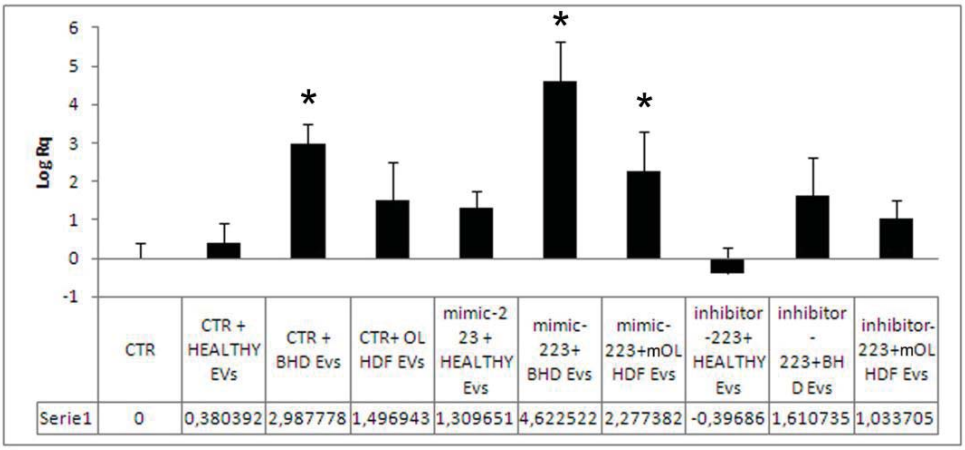

Supplementary figure 3: Levels of expression of miR-223 in all experimental conditions in the *in vitro* angiogenesis and apoptosis assays. Results are expressed as mean ± 1SD of three different experiments. AntagomiR-223 = inhibitor.

Table 1S (Supplementary Material): list of primers used for miRNA identification in plasma EV and for RUNX2 mRNA quantification in VSMC.

PRIMER	SEQUENCE
hsa-miR-17a-5p	5'- CAA AGT GCT TAC AGT GCA GGT AG -3'
hsa-miR-92a	5'- TAT TGC ACT TGT CCC GGC CTG T -3'
hsa-miR-223	5'- TGT CAG TTT GTC AAA TAC CCC A -3'
hsa-miR-423-5p	5'- TGA GGG GCA GAG AGC GAG -3'
hsa-miR-451	5'- AAA CCG TTA CCA TTA CTG AGT T -3'
hsa-RNU-48	5'- AAC TCT GAG TGT GTC GCT GAT G -3'
RUNX2 forward	5'-GAG TCC GGC CCC TCC AT-3'
RUNX2 reverse	5'-GCA ACT AAG TCA TAG TCC GCC TAG A-3'
Actin-β forward	5'-GAG TCC GGC CCC TCC AT-3'
Actin-β reverse	5'-GCA ACT AAG TCA TAG TCC GCC TAG A-3'